IOWA STATE UNIVERSITY
Digital Repository

Graduate Theses and Dissertations

Iowa State University Capstones, Theses and Dissertations

2016

Microfluidic devices for droplet sorting, on-line sensing, and microwinery

Yuncong Chen
Iowa State University

Follow this and additional works at: https://lib.dr.iastate.edu/etd

 Part of the Engineering Commons

Recommended Citation
Chen, Yuncong, "Microfluidic devices for droplet sorting, on-line sensing, and microwinery" (2016). *Graduate Theses and Dissertations*. 15680.
https://lib.dr.iastate.edu/etd/15680

This Thesis is brought to you for free and open access by the Iowa State University Capstones, Theses and Dissertations at Iowa State University Digital Repository. It has been accepted for inclusion in Graduate Theses and Dissertations by an authorized administrator of Iowa State University Digital Repository. For more information, please contact digirep@iastate.edu.

www.manaraa.com

Microfluidic devices for droplet sorting, on-line sensing, and microwinery

by

Yuncong Chen

A thesis submitted to the graduate faculty

in partial fulfillment of the requirements for the degree of

MASTER OF SCIENCE

Major: Electrical Engineering

Program of Study Committee:
Liang Dong, Co-Major Professor
Daniel Attinger, Co-Major Professor
Timothy Bigelow

Iowa State University

Ames, Iowa

2016

www.manaraa.com

DEDICATION

I would like to dedicate this thesis to my mother Guoyin and my father Bin without whose unconditional moral and financial support I would not have been able to complete this work.

www.manaraa.com

TABLE OF CONTENTS

www.manaraa.com

www.manaraa.com

LIST OF FIGURES

www.manaraa.com

www.manaraa.com

LIST OF TABLES

www.manaraa.com

ABSTRACT

Microfluidics is a promising technology that involves microsystem engineering, physics, materials, chemistry, and biotechnology. Microfluidic devices have many advantages such as small liquid volume and energy consumption, fast reaction, and good throughput of assays.

The first study of this thesis is focused on the development of a microfluidic droplet sorter able to select micro-droplet-based biochemical reactors based on their optical properties. The sorting is accomplished utilizing two bilayer pneumatic micro-valves as sorting controllers. This micro-valve, consisting of a liquid flow channel in the bottom layer, an air flow channel in the upper layer, and a flexible thin membrane in the middle layer, is a widely used building block for many large-scale integrated microfluidic systems. Rapid deflation of a pressurized micro-valve generates a fluidic pressure exerted at an optically targeted micro-droplet. This, in turn, diverts the droplet into one of multiple outlet channels. This sorter is advantageous over others by having a reduced interference to biological species or microorganisms encapsulated inside droplets and facilitating easy integration of a sorting function into large-scale microfluidic systems.

The second study aims at developing a microfluidic sensing device for improving efficiency of online concentration measurement in liquid solutions. The device integrates multiple electrical impedance-based sensors and a microfluidic concentration gradient generator onto a low-cost printed circuit board platform, to achieve a cost-effective microsystem solution. This device allows acquiring sufficient measurement data at a high concentration resolution that is generally required to create complex impedance-to-concentration mapping relationships for analyzing a multi-composition liquid solution. The Principle Component Analysis method is employed to analyze the measured data and reduce the data complexity from three to two

www.manaraa.com

dimensions. This further allows differentiating and quantifying unknown concentrations of multiple compositions in a liquid sample.

The third study involves a novel continuous flow micro-winery with a great potential to rapidly screen important parameters involved in making quality wines such as types of juice and yeast, and fermentation temperature and light conditions. This microsystem technology advances the winemaking area by reducing the fermentation time from 1-2 weeks to 1-3 days and eliminating the operation of separating wine product from yeast cells. In the device, a hydrophilic porous membrane separates a serpentine juice flow channel from a yeast storage chamber, at which yeast cells are immobilized and fermentation takes place; a hydrophobic porous membrane is additionally placed on the bottom of yeast chamber to allow escaping CO2 from the device. The immobilized yeasts, exposed to a continuous juice flow, have a higher juice-to-wine conversion rate and thus an increased fermentation efficiency.

In conclusion, this research has advanced the microfluidics area with a novel micro-droplet sorter, an online concentration measurement device, and an unprecedented microscale winery chip.

www.manaraa.com

CHAPTER 1. GENERAL INTRODUCTION

Sorting in Microfluidics

Separating and sorting micro-particles or micro-droplets from a large population is highly desirable to enhance efficiency in research and development applications. High efficiency and accuracy sorting is important for applications such as high-throughput biological assays, chemical reactions and processing, and environmental assessments. Existing sorting mechanisms can be classified as passive, active, and combined means.[1] Passive sorting utilizes interactive effects between particles/droplets, flow field and channel structures, or relies on differences in the density and size of different particles, which has a relatively low sorting efficiency.[2] For instance, the pinched flow fractionation method employs characteristics of laminar flow and difference in particle size to continuous separate particles in a channel.[3]

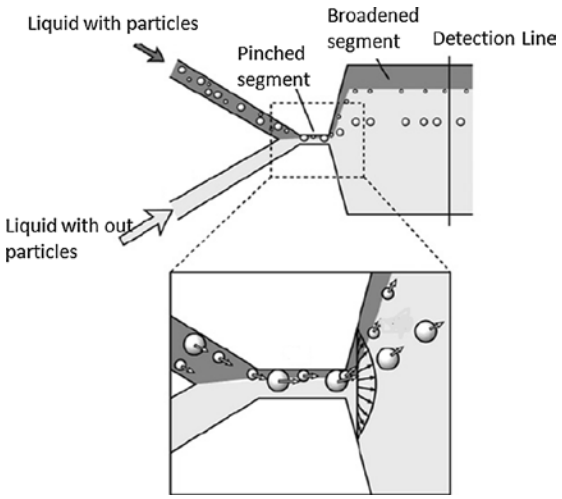

Figure 1: Schematic illustration of pinched flow fractionation (PFF) (Yamada et al. 2004)

Active sorting requires external fields, such as electric, magnetic, optical and acoustic fields, but offers higher sorting efficiency and throughput. However, these fields may have interferences on micro-bio-species and micro-organisms contained in droplets. The applied shear stress on the bio-cells may lead to damage on them when sorting is achieved based on the intrinsic properties of the bio-cells. For example, based on the differences of magnetic

www.manaraa.com

property, particles or droplets can be sorted by applying a magnetic field on the continuous flow carrying objects to be sorted.[4]

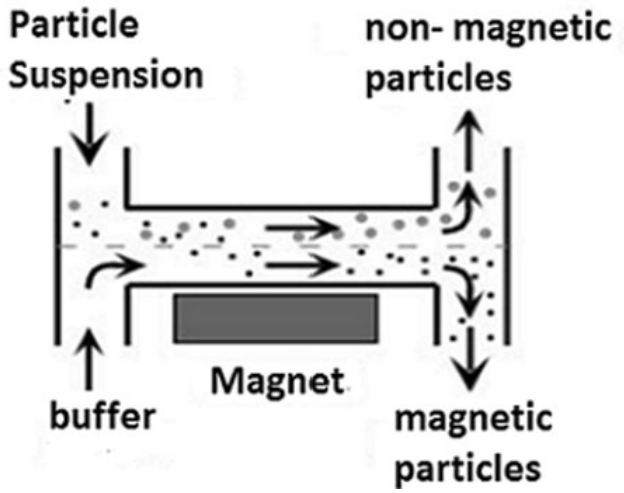

Figure 2: Continuous separation of particles (Chronis et al. 2001)

To improve sorting efficiency, some passive means of sorting also utilize external fields. Therefore, sorting techniques with easy operation, low cost, high efficiency, but no interferences on objects to be sorted is in need. We investigated a sorter utilizing pneumatic valves sorting controllers, which induce only minimal interference to biological species or microorganisms encapsulated inside droplets that may accompany electrical, optical and magnetic-based techniques.

Concentration Measurement in Microfluidics

The ability to quantify concentrations of compositions in liquid solutions is highly desirable for many applications in industrial process control, environmental monitoring, medical diagnosis, and biochemical analysis. Conventional methods such as optical spectrometry, mass spectrometry and chromatography, can provide precise concentration measurement, but require relatively expensive and bulky instruments with high maintenance and thus real-time, online monitoring is not easy to perform. Miniaturized electrical impedance

www.manaraa.com

sensors for online concentration measurement are developed by detecting changes in electrical properties of liquid samples under different concentrations. Electrical impedance spectroscopy (EIS) method has been widely applied for electrical impedance sensors to provide concentration information by measuring electrical impedances at different electrical frequencies. Therefore, impedance-to-concentration mapping relationships as a function of frequency are needed to form a reference or calibration table. A high resolution reference table for improving accuracy requires sufficient data from measurements. Thus, we investigated a microfluidic sensing device capable of a high throughput data acquisition of electrical impedance measurement to form the high resolution reference table of showing impedance-to-concentration mapping relationships of mixed solutions. The unknown concentrations of compositions in a liquid solution could be determined according to the mapping relationship by measuring the electrical impedance utilizing an electrical impedance sensor.

Miniaturized Continuous Flow Winery

Wine is typically produced in large batches, with volumes typically in the range of 10-100,000L. Grape juice is mixed with yeast, which consumes the sugars in the juice. Carbon dioxide and alcohol is released during the consumption of the sugar by the yeast, fermenting the juice to create the wine. Alcoholic fermentation occurs within one to two weeks, and the remaining winemaking operations occur within weeks to months. Yeast cells are dispersed in the juice. Monitoring of fermentation and production is done by sampling. Because of this traditional method of making wine, testing is slow and cumbersome. Sometimes, an entire batch of wine can be ruined.

Furthermore, because of the slow and lengthy process of traditional batch-style winemaking, there is little chance to adjust the variables, such as type and amount of yeast and

www.manaraa.com

grape combination, temperature of fermentation, amount of light, as well as other factors that could affect the taste, alcohol content, and other factors that determine the quality of wine produced. Climate and maturation differences vary from year to year, which makes it difficult to evaluate the effect of modifications in the winemaking process. Therefore, there is a need in the art for a quick and simple method of screening the variables of winemaking in an easier fashion to determine the best combinations for creating higher qualities of wine.

We investigated a micro-scale winey for a beverage fermenting system, which utilizes a continuous flow rather than batch approach for the fermentation of a beverage, such as a fermentation of grape juice to make wine. This is done on a miniaturized or very small scale, such as wherein the volume produced by the system may be on the order of 1ml per unit. The alcoholic fermentation can occur within one to three days, as opposed to one to two weeks, which is required for large batch alcoholic fermentation. Thus, the miniaturized, continuous flow system provided by the present disclosure will allow for greater variability in the factors that go into the fermentation of a liquid, such as yeast type, flavorings, temperature, humidity and/or some combinations thereof, to allow for greater flexibility and testing to be able to create potentially new types of fermented beverages based on the alterations of the input variables.

Thesis Organization

Chapters 2, 3 and 4 correspond to the research goals outlined above. Specifically, Chapter 2 details the research about a new means of droplet sorting. Chapter 3 describes the investigated microfluidic sensing devices for achieving improved online measurement efficiency. Chapter 4 involves an invention of miniaturized continuous-flow winery. Finally, Chapter 5 summarizes all of the conclusions drawn from the thesis and plans for future work

www.manaraa.com

in both fields. References for each chapter's contents are given at the end of the individual chapters.

References

[1] Sajeesh, P., & Sen, A. K. (2014). Particle separation and sorting in microfluidic devices: a review. Microfluidics and nanofluidics, 17(1), 1-52.

[2] Kersaudy-Kerhoas M, Dhariwal R, Desmulliez MPY (2008). Recent advances in microparticle continuous separation. IET Nanobiotechnol 2(1):1–13.

[3] Yamada M, Nakashima M, Seki M (2004). Pinched flow fractionation: continuous size separation of particles utilizing a laminar flow profile in a pinched microchannel. Anal Chem 76:5465–5471.

[4] Chronis N, Lam W, Lee L (2001) In: Ramsey JM, van den Berg A (eds) Micro total analysis system. Kluwer Academic, Monterey, p 497.

www.manaraa.com

CHAPTER 2. MICROFLUIDIC DROPLET SORTING USING INTEGRATED BILAYER MICRO-VALVES

Modified from a paper submitted to *Applied Physics Letters*

Yuncong Chen[a], Yang Tian[a], Zhen Xu, Xinran Wang, Sicong Yu, and Liang Dong[b]

Department of Electrical and Computer Engineering, Iowa State University, Ames, Iowa 50011, USA

Abstract

This paper reports on a microfluidic device capable of sorting droplets utilizing conventional bilayer pneumatic micro-valves as sorting controllers. The device consists of two micro-valves placed symmetrically on two sides of a sorting area, each on top of a branching channel at an inclined angle with respect to the main channel. Changes in transmitted light intensity, induced by varying light absorbance by each droplet, are used to divert the droplet from the sorting area into one of three outlet channels. When no valve is activated, the droplet flows into the outlet channel in the direction of the main channel. When one of the valves is triggered, the flexible membrane of valve will first be deflected. Once the droplet leaves the detection point, the deflected membrane immediately returns to its default flattened position, thereby exerting a drawing pressure on the droplet and deviating it from its original streamline to the outlet on the same side as the valve. This sorting method will be particularly suitable for numerous large-scale integrated microfluidic systems where pneumatic micro-valves are already used. Only few

[a] Y.C. and Y.T. contributed equally to this work.
[b] Author to whom correspondence should be addressed. Email: ldong@iastate.edu.

www.manaraa.com

structural modifications are needed to achieve droplet sorting capabilities in these systems. Due to the mechanical nature of diverting energy applied to droplets, the proposed sorting method may induce only minimal interference to biological species or microorganisms encapsulated inside droplets that may accompany electrical, optical and magnetic-based techniques.

Introduction

Sorting micro/nano-particles and micro-droplets from a large population with high efficiency and accuracy is highly desirable for microfluidic devices that have applications such as high-throughput biological assays, chemical reactions and processing, and environmental assessments. Existing sorting mechanisms can be classified as passive, active, and combined means[1]. Passive sorting does not require external fields, but instead utilizes interactive effects between particles/droplets, flow field and channel structures, or relies on differences in the density and size of different particles. For instance, the pinched flow fractionation method employs characteristics of laminar flow and difference in particle size to separate particles in a channel[2]. Deterministic lateral displacement is a steric method of continuous separation that makes use of asymmetric bifurcation of laminar flow around obstacles[3]. In contrast, active sorting requires external fields in various forms and offers higher sorting accuracy. Remarkable active means of sorting include using dielectrophoresis under electric fields[4,5], and applying magnetic fields to differentiate particles based on their magnetic properties[6,7]. Optical, acoustic, and mechanical methods have also been used to achieve sorting[8-13]. To improve sorting efficiency, some passive means of sorting also utilize external fields[14-16]. A modification to the pinched flow fractionation method involves applying a laser beam to particles for improved sorting efficiency[15,16].

Notably, the pneumatic micro-valve developed by Quake et al.[17] has become a widely used on-chip valving method in many biochip applications. This valve involves a bilayer

www.manaraa.com

polydimethylsiloxane (PDMS) structure, where liquid flows inside the bottom layer while the upper layer integrates an air network. Between the bottom and upper layers is a thin flexible membrane. To activate the valve, compressed air is pumped into the air channel such that the membrane is forced to bend towards the liquid flow channel. This operation allows compressing and clogging of channels in the fluidic layer to manipulate liquid flow. Such valves have been extensively utilized as active components to perform valving, chopping, switching, and pumping[18,19] in integrated microfluidic systems[17].

In this paper, we report a new means of sorting micro-droplets utilizing bilayer pneumatic micro-valves. The proposed droplet sorter shown in Fig. 3a consists of a main inlet channel and three outlet channels. Two valves, i.e., V1 and V2, are placed on two side-channels at an inclined angle with respect to the main channel, serving as sorting controllers. These channels meet at a droplet sorting area. The two control valves are set to be normally opened with flat membranes. An optical detection setup is used to determine the direction of diverting a target droplet away from the sorting area into one of three outlet channels, where a laser beam originating from the top of the device is aimed a detection spot (indicated by green circle in Fig. 3a) located at the end of the main channel near the sorting area (indicated by a dashed red circle). When a droplet in Fig. 3b arrives at the detection point from the main channel, it attenuates transmitted light signals based on its light absorbance and/or scattering characteristics. The transmitted light intensity (TLI) is detected by a photodetector on the lower side of the sorter. If the change in the TLI is more than a pre-determined trigger value, then a valve will be triggered to turn on and pneumatically deflect the membrane (Fig. 3c). In this moment, the droplet movement is not deviated from the streamline yet because it still remains in the main channel. However, once the droplet leaves the detection point and immediately enters the sorting area, the change in the TLI will become less than the pre-

www.manaraa.com

set value. As a result, the valve will be deflated and the membrane will return upward to its default flattened position, thereby exerting a drawing force on the droplet (Fig. 3d). The droplet will thus deviate from its original streamline to flow into the collection channel on the same side as the activated valve (Fig. 3e). Therefore, by pre-setting two different trigger values for the two valves, droplets with different light absorbance and scattering characteristics can be diverted to either outlet O1 or O3. Without any operations of the valves, the droplets-containing flow coming from the main channel will enter into outlet O2 oriented along the main channel.

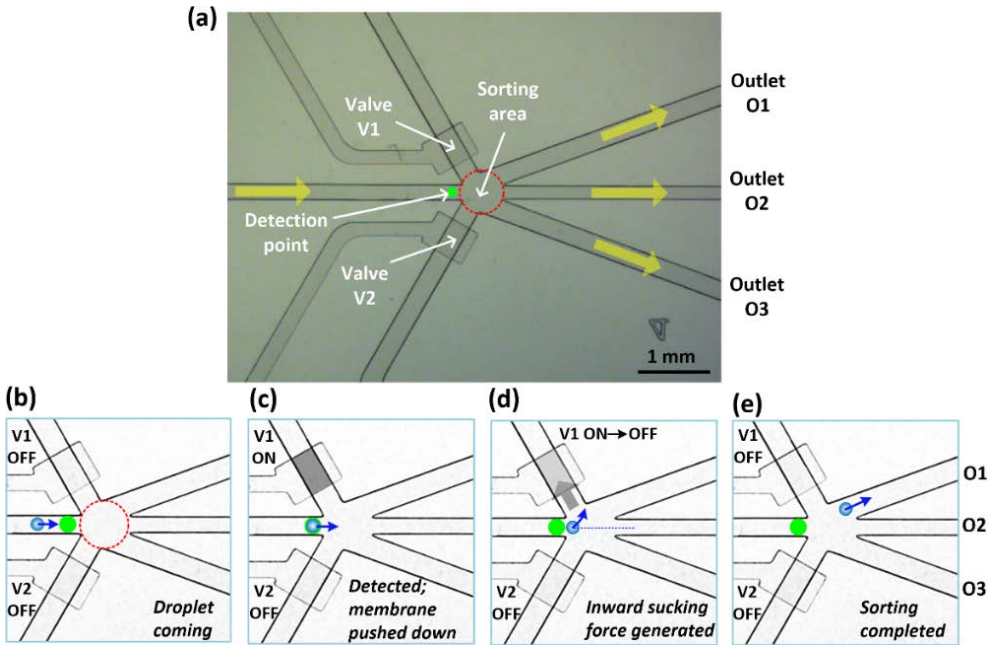

Figure 3: (a) Photograph of the proposed micro-droplet sorter. The green dot and the dashed red circle represent the optical detection point and the sorting area, respectively. (b)–(d) Schematic of the sorting processes. The blue dot represents a target water droplet carried by an oil phase flow. The gray arrow in (d) at the valve represents the inward drawing pressure generated during the relaxation of the deflected membrane.

Experimental Setup and Simulation

A finite element method based on COMSOL Multiphysics software (Burlington, USA) was used to illustrate the proposed sorting mechanism. The geometrical and dimensional parameters were set to be the same as those used in the fabricated device made of PDMS with a 50 μm-deep fluid channel layer on the bottom, a 200 μm-deep air control layer on the top, and a sandwiched 25 μm-thick membrane layer. Water droplets were considered to be carried

www.manaraa.com

downstream by a continuous silicone oil flow with a density and viscosity of 0.967×10^{3} kg·m^{-3} and 9.3×10^{-3} Pa·s, respectively. The flow velocity was set to be 2.2×10^{-3} m·s^{-1}. The pressures at three outlets were all set to an atmospheric pressure of 1.01×10^{5} Pa. The valves were initially in the "on" state with an applied pressure of 6.9×10^{5} Pa from a compressed air source. Thus, as the valve returned to its default flat position, the generated drawing pressure was assumed to be -6.9×10^{5} Pa. The simulation results in Fig. 4 illustrate how the flow direction can be controlled by the two valves. When both of the valves are in the off state (flat membrane), the middle outlet O2 has the lowest pressure (Fig. 4a) and thus the main flow is directed towards this outlet (Fig. 4d). When valve V1 is triggered to be on and then immediately off, an inward drawing pressure is generated in the sorting area (Fig. 4b), thus diverting the flow to outlet 1 (Fig. 4e). Similarly, the flow can be diverted to outlet 3 (Fig. 4f) when valve V2 in Fig. 4c is triggered to operate in the same way as V1 in Fig. 4b.

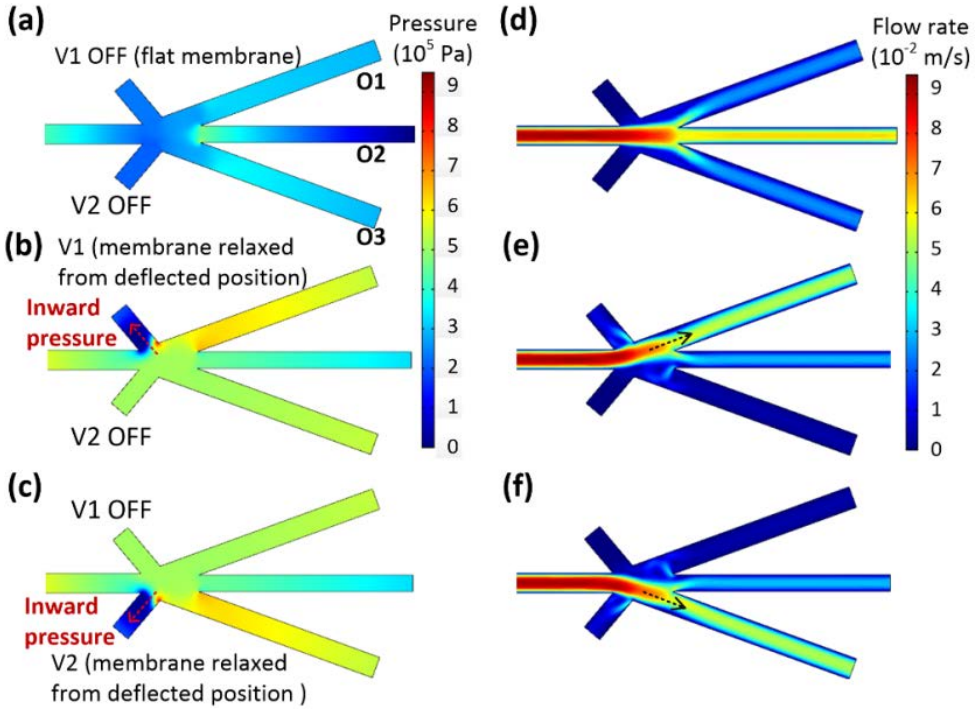

Figure 4: Hydrodynamic simulations for (a)–(c) fluidic pressure and (d)–(f) corresponding flow rate distributions of water in the proposed sorter.

www.manaraa.com

Figure 5a shows the setup of the sorting system. Electrically activated solenoids (S10MM-31-12-3/A; Pneumadyne, Plymouth, MN) were used to control the valves. The solenoids were connected to a compressed air source and fed by the electrical signal output of the photodetector. To generate droplets with different optical properties, the microfluidic device contained an alternating droplet generator (ADG)[20] with two cross-junction droplet generation units at the upstream end of the main channel (Fig. 5b). Figure 5c shows the electronic circuit that amplifies the signals from the photodetector and then compares them with the pre-set trigger voltages. In our experiments, three different water solutions were prepared by mixing black food-dye solution (AmeriColor) with deionized (DI) at different volume ratios of 10%, 5%, and 0.5%. Single color droplets were produced by one generation unit on the ADG, while generating droplets with two different colors required use of both generation units. The fabrication processes for the PDMS sorter is described in the Supplementary Material[21].

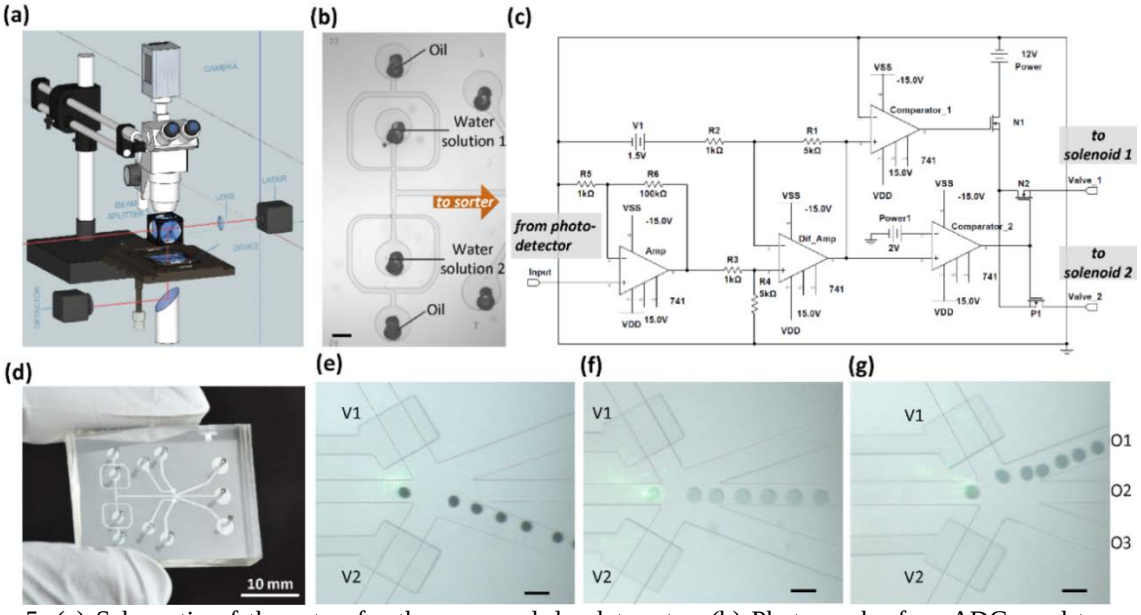

Figure 5: (a) Schematic of the setup for the proposed droplet sorter. (b) Photograph of an ADG used to produce different color droplets to test the sorter. The scale bar represents 700 µm. (c) Electronic circuit used to control the states of the valves. (d) Photograph of the sorter. (e)–(g) Directing a train of droplets with the same color into different outlet channels based on the gray level of the droplets: dark (e), light (f), and mediate (g) levels. The scale bars represent 300 µm.

www.manaraa.com

Results and Discussion

We first assessed the ability of the sorter to direct a train of droplets with the same color into a designated outlet. The pre-set trigger voltages at the output of the amplifier circuit for driving valves V1 and V2 were 1.8 V and 1.2 V, respectively. When no droplets flowed through the detection area, the output voltage was 2.4 V. In Fig. 5e, when the dark droplets passed through the detection point, the output voltage value decreased to lower than 1.2 V, constituting a 54 % reduction in the TLI, and thus V2 was triggered to divert the droplets into outlet O3, while V1 remained in the "off" state. As another train of light droplets in Fig. 5f flowed through the detection point, the resulting 12% reduction in the TLI was not significant enough to bring the output voltage below 1.8 V, and thus no valves were triggered. As a result, the light droplets flowed downstream into outlet O2 (Fig. 5f). When the mediate color droplets arrived at the sorting area, a 31% reduction in the TLI occurred, which caused the voltage to decrease to 1.5 V, thus triggering V2 but not V1. As expected, the mediate color droplets were directed to outlet O1 (Fig. 5g).

Next, we investigated whether or not the sorter could extract desired droplets from a stream of droplets with mixed colors. Figure 6a shows droplets of two gray levels were produced by the ADG and alternatively flowed into the main channel. Figure 6b shows that the mediate color droplets were directed by valve V2 into outlet O1, while the light color droplets continued flowing into outlet O2 in the middle. Figure 6c shows that the dark droplets were redirected by V1 and flowed into outlet O3, while the light ones flowed into the middle outlet channel O2. The images in Fig. 6 were extracted from the movies available in Supplementary Material.[21] In this experiment, the pre-set voltages for triggering V1 and V2 were the same as those of the previous experiment at 1.8 V and 1.2 V, respectively. To visualize each critical step of the entire sorting process, detailed decompositions are provided in Fig. 6d. A mediate color droplet (indicate by a red arrow)

www.manaraa.com

arrived at the detection point at 20 ms, triggering the initially flat membrane of V1 to deflect downward. Once the droplet left the detection point, the membrane returned flat to draw the droplet towards the valve at 40 ms, during which the droplet was deformed by the drawing pressure. Almost at the same time, a light color droplet (indicated by a blue arrow) arrived at the detection point. But, none of the valves were triggered owing to the inadequate change in the TLI at 60 ms. Thus, this droplet did not deviate from its original flow direction, and entered outlet O2 at 80 ms. At this time, the initial droplet had already flowed inside the channel of outlet O1.

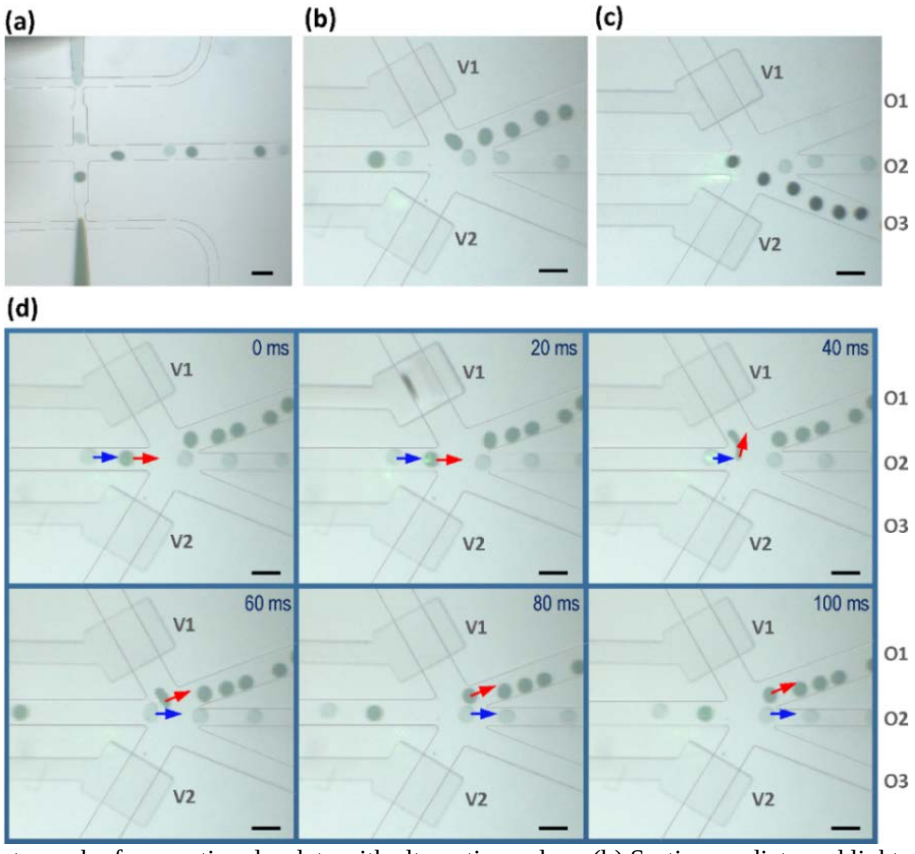

Figure 6: (a) Photograph of generating droplets with alternating colors. (b) Sorting mediate and light color droplets to outlet O1 and O2, respectively. (c) Sorting light and dark color droplets to outlet O2 and O3, respectively. (d) Time-lapse images for sorting a mediate color droplet (indicated by a red arrow) to outlet O1, and the following light droplet (blue arrow) to outlet O2. The scale bars represent 300 μm.

In the experiments described above, the detection point was located at the end of the main channel and the inward sucking pressure was created from the relaxation of the deflected valve membrane and exerted upon a target droplet for sorting. In another trial shown in Fig. 7, the

www.manaraa.com

detection point was relocated into the sorting area and the outward pushing pressure generated during the downward deflection of the membrane was instead used to divert a target droplet. The results show that when a mediate color droplet entered the sorting area, valve V2 was triggered to deflect its membrane pushing away the droplet (Figs. 7a, 7b and Figs. 7e, 7f). But, after the droplet left the detection point, the membrane of V2 immediately returned upward to the flat position, during which the accompanying sucking pressure by V2 was applied to the droplet, thus drawing it backwards (Figs. 7c, 7g). Therefore, the droplet in Figs. 7d and 7h was incorrectly directed into outlet O2. Similarly, an inward sucking pressure generated during the relaxation of the deflected membrane also failed to draw a target droplet into the outlet on the same side of the valve. Therefore, this mode of operation in Fig. 7 would not be recommended to use in sorting.

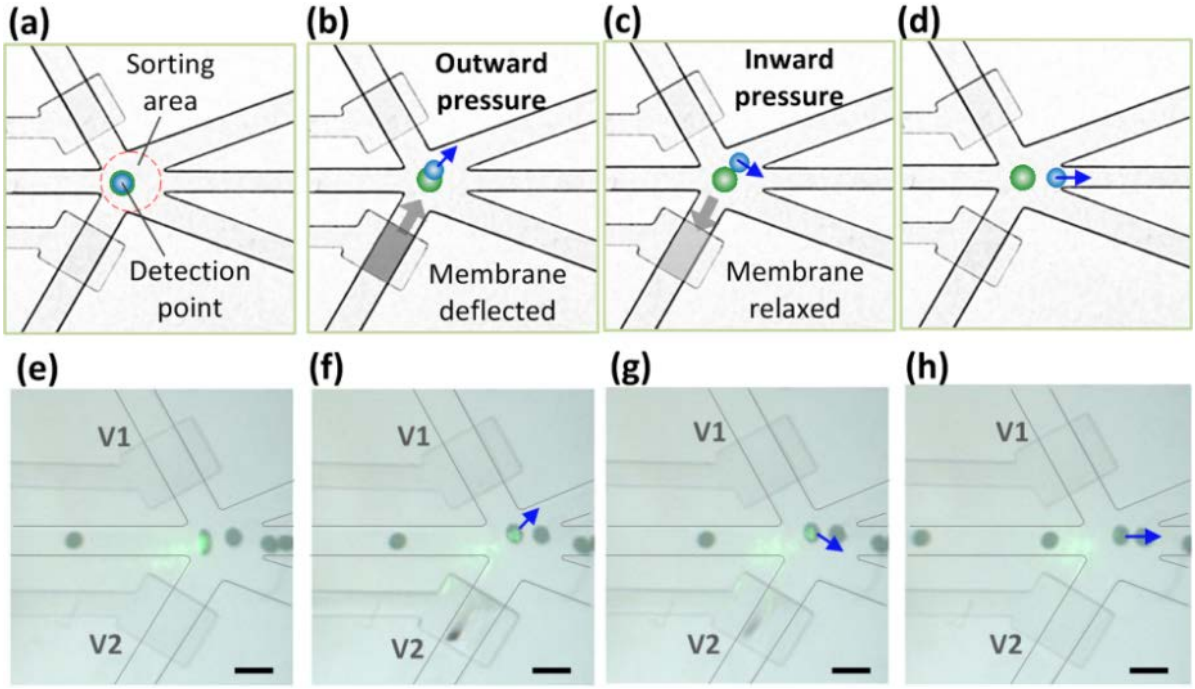

Figure 7: (a)–(d) Decompositions of droplet sorting based on using the outward pressure to drive a target droplet into a desired outlet channel. The detection point was located in the sorting area. (e)–(d) Time-lapse images of droplet sorting correspondingly described in (a)–(d). In (f), the outward pressure was generated as the membrane of V1 was deflected downward. In (c), before the droplet completely left the detection area, the inward pressure generated during the relaxation of the membrane pulled the droplet back to the sorting area. The scale bars represent 300 μm.

www.manaraa.com

Fig. 8 shows that the proposed droplet sorter was capable of achieving an almost 100% success rate when sorting frequency was no more than f = 20 Hz. Here, sorting frequency is defined as the number of droplets passing through the detection point within one second. As the sorting frequency further increased, the success rate of sorting decreased. At f = 25 Hz, the sorting error rate was ~12%. Although the detection electronics of the system provided a microsecond-scale response time, the pneumatic valve was not fast enough to correctly respond to an operation instruction by switching between its "on" and "off" states at a higher sorting frequency. Compared to previously reported two mechanical sorters using vertical wall based in-plane pneumatic valves[12,13], our bilayer valve based sorter provided a higher sorting frequency than the one with five sampling outlets (~2 Hz)[12], but lower than the other with two sampling outlets (~250 Hz)[13]. The moderate sorting frequency of our sorter may perhaps be caused by the indirect body contact of the droplets with the valves and the moderate number of sampling outlets. It should be noted that although the in-plane pneumatic valves have a simpler structure[22], each valve often requires an individual control, which may cause complexity in designing large-scale microfluidic systems[23] with multiple sorters and other units. In contrast, the bilayer valves adopted in our sorter need relatively complex fabrication processes, but, they are known for addressable control to reduce layout complexity of pneumatic lines used in microfluidic large-scale integration[17,23]. Therefore, the proposed sorter will be particularly suitable for integration into complex microfluidic systems that use pneumatic bilayer valves[17,23]. With only a few structural modifications, droplet sorting capabilities, when needed, will be readily achieved in these systems.

www.manaraa.com

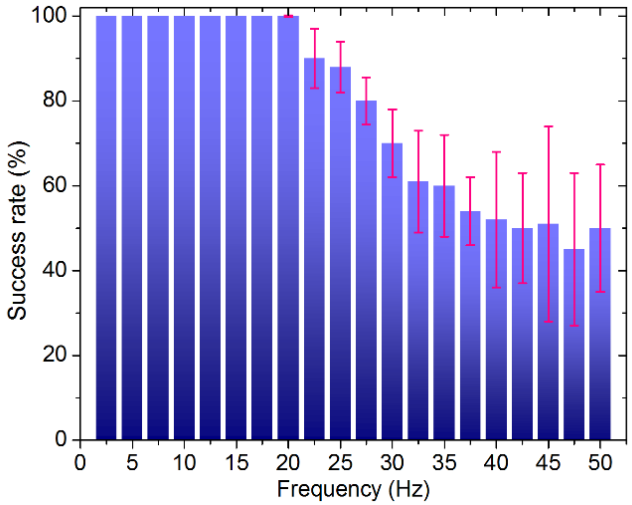

Figure 8: Sorting error analysis based sorting success rate as a function of sorting frequency. Error bars represent standard deviation obtained from sorting 10^3 droplets.

Conclusion

The potential applications of the proposed microfluidic droplet sorter are widespread since the mechanical means of droplet sorting may induce minimal interference to biological species or microorganisms encapsulated inside droplets that often accompany many other active separation and sorting devices using electrical, optical and magnetic driving forces. Future work includes applying this microfluidic sorter to sort droplets containing cells whose growth density may influence the TLI and thus trigger sorting. It is also our interest to integrate this sorting method with other sensing mechanisms such as fluorescence detection, to develop a flow cytometer-like device for sorting droplets.

Acknowledgements

This work was supported in part by the Plant Sciences Institute and the Institute for Physical Research and Technology at Iowa State University, and the National Science Foundation under grants # ECCS-1102354, ECCS-0954765 and DBI-1353819. The authors also thank Dr. Zhiyou Wen and Dr. Laura Jarboe for their helpful discussions.

www.manaraa.com

References

[1] P. Sajeesh and A. K. Sen, "Particle separation and sorting in microfluidic devices: a review," Microfluid. Nanofluidics **17**, 1-52 (2014).

[2] J. Oakey, J. Allely, and D. W. Marr, "Laminar-flow-based separations at the microscale," Biotechnol. Prog. **18**, 1439-1442 (2002).

[3] L. R. Huang, E. C. Cox, R. H. Austin, and J. C. Sturm, "Continuous particle separation through deterministic lateral displacement," Science **304**, 987-990 (2004).

[4] X. B. Wang, Y. Huang, F. F. Becker, and P. R. C. Gascoyne, "A unified theory of dielectrophoresis and travelling wave dielectrophoresis,"J. Phys. D Appl. Phys. **27**, 1571 (1994).

[5] X. B. Wang, J. Yang, Y. Huang, J. Vykoukal, F. F. Becker, and P. R. C. Gascoyne, "Cell separation by dielectrophoretic field-flow-fractionation," Anal. Chem. **72**, 832-839 (2000).

[6] K. Smistrup, T. Lund-Olesen, M. F. Hansen, and P. T. Tang, "Microfluidic magnetic separator using an array of soft magnetic elements," J. Appl. Phys. **99**, 08P102 (2006).

[7] M. Bu, T. B. Christensen, K. Smistrup, A. Wolff, and M. F. Hansen, "Characterization of a microfluidic magnetic bead separator for high-throughput applications," Sensor. Actuat. A Phys. **145**, 430-436 (2008).

[8] O. Brzobohatý, V. Karásek, M. Šiler, L. Chvátal, T. Čižmár, and P. Zemánek, "Experimental demonstration of optical transport, sorting and self-arrangement using a 'tractor beam'," Nat. Photonics **7**, 123-127 (2013).

[9] A. Lenshof, C. Magnusson, and T. Laurell, "Acoustofluidics 8: Applications of acoustophoresis in continuous flow microsystems," Lab Chip **12**, 1210-1223 (2012).

[10] S. Li, X. Ding, F. Guo, Y. Chen, M. I. Lapsley, S. C. S. Lin, W. Lin, J. P. McCoy, C. E. Cameron and T. J. Huang, "An on-chip, multichannel droplet sorter using standing surface acoustic waves," Anal. Chem. **85**, 5468-5474 (2013).

[11] Q. Zhang, P. R. Zhang, Y. T. Su, M. L. Yang, and B. Ma, "On-demand control of microfluidic flow via capillary-tuned solenoid microvalve suction," Lab Chip **14**, 4599-4603 (2014).

[12] D. H. Yoon, D. Wakui, A. Nakahara, T. Sekiguchi, and S. Shoji, "Selective droplet sampling using a minimum number of horizontal pneumatic actuators in a high aspect ratio and highly flexible PDMS device," RSC Adv. **5**, 2070-2074 (2015).

[13] A. R. Abate, J. J. Agresti, and D. A. Weitz, "Microfluidic sorting with high-speed single-layer membrane valves," Appl. Phys. Lett. **96**, 203509 (2010).

www.manaraa.com

[14] Z. Wu, A. Q. Liu, and K. Hjort, "Microfluidic continuous particle/cell separation via electroosmotic-flow-tuned hydrodynamic spreading," J. Micromech. Microeng. **17**, 1992. (2007)

[15] A. Y. Lau, L. P. Lee, and J. W. Chan, "An integrated optofluidic platform for Raman-activated cell sorting," Lab Chip **8**, 1116-1120 (2008).

[16] K. H. Lee, S. B. Kim, K. S. Lee, and H. J. Sung, "Enhancement by optical force of separation in pinched flow fractionation," Lab Chip **11**, 354-357 (2011).

[17] M. A. Unger, H. P. Chou, T. Thorsen, A. Scherer, and S. R. Quake, "Monolithic microfabricated valves and pumps by multilayer soft lithography," Science **288**, 113-116 (2000).

[18] C. W. Lai, Y. H. Lin, and G. B. Lee, "A microfluidic chip for formation and collection of emulsion droplets utilizing active pneumatic micro-choppers and micro-switches," Biomed. Microdevices **10**, 749-756 (2008).

[19] O. C. Jeong, and S. Konishi, "Fabrication and drive test of pneumatic PDMS micro pump," Sensor. Actuat. A Phys. **135**, 849-856 (2007).

[20] D. R. Link, E. Grasland-Mongrain, A. Duri, F. Sarrazin, Z. Cheng, G. Cristobal, M. Marquez, and D. A. Weitz, "Electric control of droplets in microfluidic devices,"Angew. Chem. Int. Ed. **45**, 2556-2560 (2006).

[21] See supplementary material at http:// , including the fabrication processes for the microfluidic sorter and three movies showing the sorting processes.

[22] A. R. Abate, M. B. Romanowsky, J. J. Agresti, and D. A. Weitz, "Valve-based flow focusing for drop formation," Appl. Phys. Lett. **94**, 023503 (2009).

[23] T. Thorsen, S. J. Maerkl, and S. R. Quake, "Microfluidic large-scale integration," Science **298**, 580-584 (2002).

www.manaraa.com

CHAPTER 3. MICROFLUIDIC IMPEDANCE SENSOR ARRAYS INTEGRATED ON PRINTED CIRCUIT BOARD FOR IMPROVED ONLINE MEASUREMENT EFFICIENCY

Modified from a paper to be submitted to *IEEE Sensors Journal*

Yuncong Chen,[1] Zhen Xu,[1] Shawana Tabassum,[1] Xinran Wang,[1] Daniel Attinger,[2] and Liang Dong[1,*]

[1]Department of Electrical and Computer Engineering, Iowa State University, Ames, Iowa 50011, USA

[2]Department of Mechanical Engineering, Iowa State University, Ames, Iowa 50011, USA

Abstract

Concentrations determination of compositions in a liquid solution is very important in numerous fields. Many analytical technologies have been investigated such as spectrometric, mass spectrometric and chromatographic techniques, but most competing techniques require costly instruments and not allowed for online measurement. Electrical impedance sensor is a low cost sensor enables monitoring real-time information, but sufficient data is needed for discovering the impedance-to-concentration mapping relationship for mixed solutions. This paper reports on an electrical impedance sensing device capable of high-throughput analyzing concentrations of compositions in liquid, for building the mapping relationship between impedances and

[a)] Author to whom correspondence should be addressed. Email: ldong@iastate.edu; Tel: +1-515-294-0388.

www.manaraa.com

concentrations. The device consists of a microfluidic concentration gradient generator integrated on a printed circuit board (PCB), where a circuit with interdigitated electrodes (IDE) arrays pre-fabricated on it. The IDE arrays are directly patterned on a PCB platform to form a substrate. The microfluidic concentration gradient generator is bonded on the PCB substrate and used for efficient generation of mixed solutions with different concentrations of compositions. The electrical impedance at each outlet is measured by its corresponding IDE array. An impedance-to-concentration mapping relationship can be discovered by measuring different combinations of solutes prepared by the concentration gradient generator. The Principle Component Analysis (PCA) is applied to analyze the data. Thus, each composition's concentration in an unknown liquid sample could be determined according to the mapping relationship by measuring the electrical impedance utilizing an electrical impedance sensor. An application of this microfluidic device for winemaking measurement is demonstrated at last.

Introduction

The ability to quantify concentrations of compositions in liquid solutions is highly desirable for many applications such as industrial process control, environmental monitoring, medical diagnosis, and biochemical analysis. Optical spectrometry[1], mass spectrometry[2] and chromatography[3] can provide precise concentration measurement, but these methods require relatively expensive and bulky instruments with high maintenance and thus real-time, online monitoring is not easy to perform. Numerous miniaturized sensors are available for concentration measurement by detecting changes in optical and electrical properties of liquid samples under different concentrations. Among these miniaturized sensors, optical sensors are able to quantify their absorbance[4], reflectance[5], transmittance, or resonant wavelength[6] when exposed to different concentrations of solutions and need light sources, detectors, and other optical components, which

www.manaraa.com

are often difficult to integrate with the sensor chip toward a compact system. In contrast, electronic sensors for determining solution concentrations based on electrical impedance measurement feature a simple structure consisting of a pair of electrodes favorable to be made with other electronic processing circuits on a single platform[7]. Electrical impedance spectroscopy (EIS) method has been widely applied for electrical impedance sensors to provide concentration information at different electrical frequencies.[8,9] This method is able to identify and separate different contributions to electric and dielectric responses of materials under different frequencies, and thus is useful for determining concentrations of main compositions in a liquid mixture. The general approach of EIS is to measure the electrical impedance of a sample as a function of the frequency by applying an electrical stimulus to the electrodes of an impedance sensor and then obtain responding voltage or current output signals under difference frequencies. Therefore, impedance-to-concentration mapping relationships as a function of frequency are needed to form a reference or calibration table. The table often has multidimensional datasets, including real and imaginary parts of impedance at different concentrations of chemicals, and corresponding frequencies. To simply the analysis, notable pattern algorithms such as Principle Component Analysis[10] (PCA) or Artificial Neural Network[11] can be utilized. For example, the PCA is able to simplify the multidimensional datasets into two principle components, i.e., PC1 and PC2, without loss of critical information, which makes the mapping relationship more straightforward with only PC1 and PC2 for different concentrations of chemicals in a table. Therefore, the table allows the users to quantify unknown concentrations of compositions in a sample can be determined.

To enhance the accuracy of PCA analysis for mixed solutions, impedance-to-concentration mapping tables with sufficient data and high concentration resolution are needed. Furthermore, different combinations of multiple components in the samples as a function of concentrations need

www.manaraa.com

to be calibrated. In this paper, we investigated an integrated microfluidic device providing high concentration resolution and good data acquisition throughput for generating impedance-to-concentration mapping tables. The microfluidic device is formed on a printed circuit board (PCB) consisting of an array of interdigitated electrodes (IDE) based impedance sensors[12], a microfluidic concentration gradient generator (CGG)[13,14], and an electronic addressing and readout circuit. Liquid solutions with different concentrations of compositions are generated at outlets of the microfluidic CGG where IDE sensors are formed. These sensors are individually addressed by the electronic circuits and their impedances are read out using an impedance meter. Therefore, rapid production of impedance measurements for sets of solution concentrations can be achieved. To validate the utility of the microfluidic device, different concentrations and combinations of ethanol, L-malic acid and L-tartaric acid, which serve main constituents of grape wine, are automatically prepared using the microfluidic CGG, and their influences on electrical impedances of the IDE sensor array are obtained using the device and analyzed using the PCA. In grape wine, L-tartaric acid and L-malic acid present 70–90% of total grape acidity, ethanol concentration indicates the alcohol percentage. The impedance characteristics of differently combined concentrations of ethanol, L-malic acid and L-tartaric acid are well calibrated, which make the device useful for grape wine quality evaluation and winemaking process monitoring[15].

Device Design and Fabrication

Design Considerations

The proposed microfluidic device in Fig. 9a consists of a microfluidic CGG with four inlets and eight outlet channels, eight IDE sensors formed at the outlet channels of the CGG, and an electronic circuit. All of these components are fabricated on a PCB to reduce cost of the device. Each sensing element is located beneath an outlet channel. Between the CGG and the IDEs is a

www.manaraa.com

thin polydimethylsiloxane (PDMS) membrane. The electronic circuit contains multiplexers to select a sensing element and set up its measurement timing and duration. The selected sensor is connected to an impedance meter for signal readout.

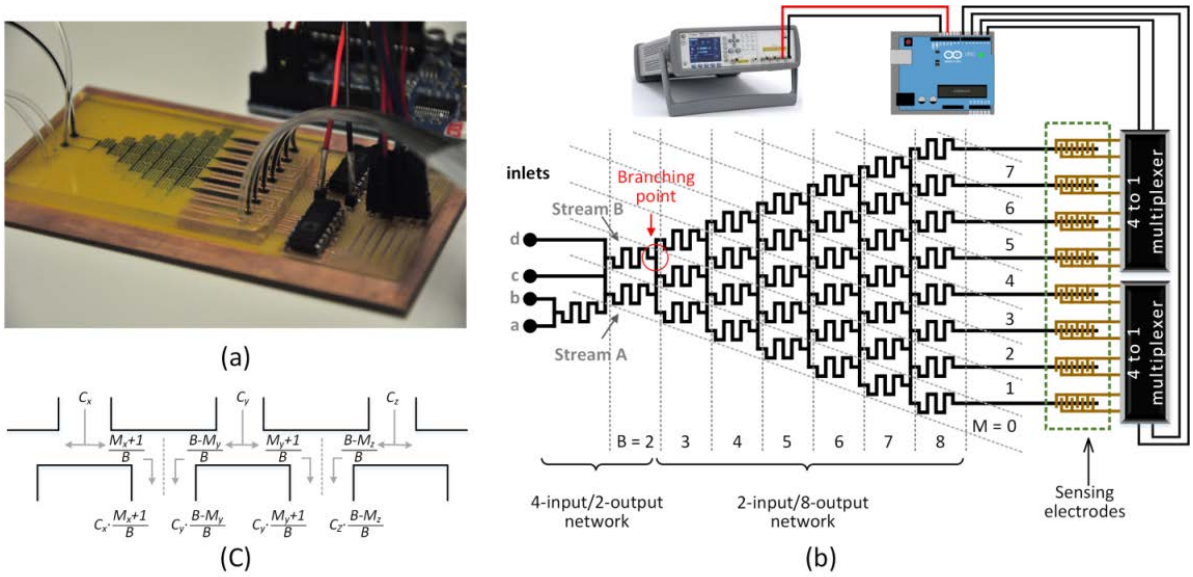

Figure 9: (a) Photo of the fabricated microfluidic device on a PCB. (b) Schematic of the device set-up, including the microfluidic CGG, the IDE array, and the impedance meter. (c) Schematic of the splitting ratio at the branching points of the microfluidic CGG, where C_x, C_y and C_z represent concentrations of three up streams.

The interdigitated design of detection electrodes allows increasing impedance changes at a limited sensing area of the outlet channel. By designing the array of eight IDE pairs on the device, eight impedance measurements for different concentrations and/or combinations can be achieved almost simultaneously, thus obtaining a higher measurement throughput with much lower sample consumption than that using conventional large reactors. To avoid possible erosion on the electrodes due to direct exposure to chemical solutions, a thin PDMS layer is coated on the surface of electrodes, serving as a physical barrier between the IDEs and the solutions, but a dielectric medium for the IDEs. This protects the IDEs from being chemically attacked, thus making long-term use of the device possible. The alternating current signal can pass through the thin PDMS layer to perform impedance measurement.

www.manaraa.com

The microfluidic CGG is also made of PDMS on the top surface of PCB. The channels of the CGG are 600 μm deep and 200 μm wide. The CGG is comprised of two parts: an upstream mixer having four inputs (see labels "a", "b", "c" and "d" in Fig. 9b) and two outputs (see labels "A" and "B" in Fig. 9b) for initial solution preparation, and a downstream mixing network having two inputs ("A" and "B") and eight outputs ("M0" – "M7") for generating concentration gradients of chemicals. We define the 2-input/8-output mixing network contains *n* mixer modules as a branched system of Bth order. Mixer modules are labeled from bottom to top as start from M = 0 and end up with M = B - 1. The branching point is at the end of each mixer module. Since each mixer module has the same dimensions, the resistivity for fluid flowing through mixer modules is the same. Furthermore, the same length of the horizontal channels at branching point leads to a same resistivity for fluid. As a result, when the input flow rates of stream A and B are the same, the flux of liquid from upstream to a branching point distributes equally, leading the flux through each mixer module to be equal. The splitting ratios of a stream that turns to the left and to the right (Φ_left and Φ_right) are given by Eq. (1) and (2), respectively.[16]

$$\Phi\_left = (B - M) / B \quad (1)$$

$$\Phi\_right = (M + 1) / B \quad (2)$$

These two splitting ratios are used to characterize the concentration change when a stream is diluted by its neighboring stream at the branching point (Fig. 9c). Thus, in the 2-input/8-output network, the solution concentrations at the outlets can then be estimated in functions of concentrations of stream A and B (C_A and C_B): 100% C_A, $\frac{1}{7}C_A + \frac{6}{7}C_B$, $\frac{2}{7}C_A + \frac{5}{7}C_B$, $\frac{3}{7}C_A + \frac{4}{7}C_B$, $\frac{4}{7}C_A + \frac{3}{7}C_B$, $\frac{5}{7}C_A + \frac{2}{7}C_B$, $\frac{6}{7}C_A + \frac{1}{7}C_B$, and 100% C_B, respectively. The concentrations of the four compositions appearing in stream "A" and "B" are determined by the flow rate of the pure solutions injected at the four inlets "a", "b", "c" and "d" during the initial solution preparation following the same ratios

www.manaraa.com

of splitting rule above. The mixed solution flow rate from inlets "a" and "b" (defined as Q_{a+b}) is set equals to the solution flow rate from inlet "d" (Q_d), leading to the flux from inlet "c" splits into two equal parts at the branching point. Setting the flow rate of injected solution from inlet "c" , Q_c, equals to two times Q_d and Q_{a+b}, the split half flux has the same flow rate as Q_c and Q_{a+b}. As a result, the mixed solution from inlets "a" and "b" contributes 50% flux to stream A, and half of the solution from inlet "c" contributes 50% flux to stream A; the other half of the solution from inlet "c" contributes 50% flux to stream B, and the solution from inlet "c" contributes 50% flux to stream B. The concentration of stream A equals to 50% of mixture's concentration from inlets "a" and "b", plus 50% of solution's concentration from inlet "c"; The concentration of stream B equals to 50% of solution's concentration from inlet "c", plus 50% of solution's concentration from inlet "d". Therefore, the output concentrations of chemicals at eight outlets of the microfluidic CGG can be estimated as a function of concentrations of solutions from inlets "a", "b", "c" and "d".

The PCB used here is a 1.6 mm-thick FR4 PCB and has a dielectric constant of 4.5. The copper layer on the board is 70 μm thick. Each finger of the electrodes is 250 μm wide and 2.4 mm long, and the gap distance between neighboring fingers is 250 μm wide (Fig. 10a). Fig. 10b gives the equivalent circuit model of the proposed electrical impedance sensor. The parasitic capacitance C_p due to the direct coupling between two neighboring electrodes is considered in this model. The thin PDMS film between the carrying fluids and the electrodes acts as a dielectric material rendering a capacitance of C_{PDMS} between each electrode and the fluid in the channel. Therefore, the input impedance of the sensor can be written as:

$$Z_{in} = \frac{1}{j\omega C_p} \cdot \frac{j\omega + \frac{2}{Z_{channel} C_{PDMS}}}{j\omega + \frac{1}{Z_{channel}} \cdot \left(\frac{1}{C_p} + \frac{2}{C_{PDMS}}\right)} \tag{3}$$

Where ω is the angular frequency of applied AC signal and $Z_{channel}$ is the impedance of the microfluidic channel. The dielectric constant of PDMS is 2.8 at 20°C. Since the liquid flow channel

www.manaraa.com

is 2 mm wide, the Area of the formed capacitor is 3.5×10^{-6} m^2. The PDMS film is 0.1 mm thick, thus the capacitance of between one electrode and the liquid flow channel C_{PDMS} equal to 8.677 pF. C_p can be calculated according to the gap distance between neighboring fingers, which equals to 0.117 pF. When no solution flows inside the channel, $Z_{channel}$ is a pure capacitance of air; when a solution flows inside the channel, $Z_{channel}$ equals to the impedance of the solution. Fig. 10c shows the calculated impedance of the sensor with air or water flowing in the channel based on the circuit model in Fig. 10b, and the measured impedances of the eight sensing elements with air or water flowing in the channel as a function frequency changing from 50 Hz to 100k Hz. In this experiment, the impedances of eight sensors are similar and close to the simulated model, thus each sensor was made relatively uniform as we expected from the model.

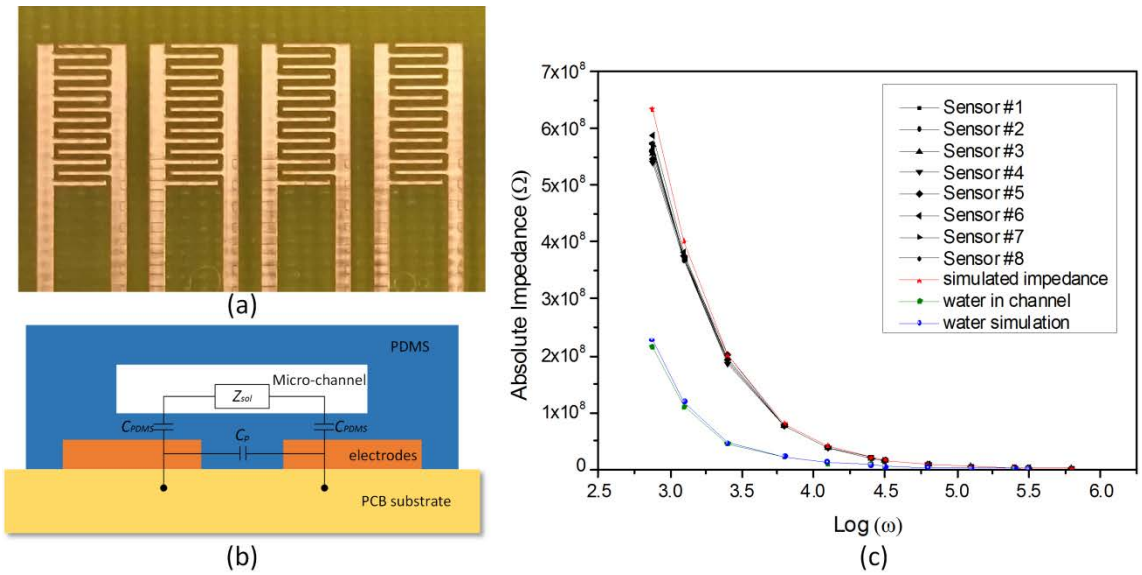

Figure 10: (a) Top view of electrodes sensor. (b) Equivalent circuit model of the proposed electrical impedance sensor with liquid solution flow in the channel (not to the scale). (c) Measured impedances of eight sensors compared with simulated impedance of equivalent model.

Device Fabrication

Fig. 11 shows the process flow for manufacturing the proposed device. First, a PCB containing an array of eight identical IDEs and other circuit geometries was designed using an electronic design automation software system (Advanced Design System), and then was fabricated

www.manaraa.com

in the top copper layer of the board using a circuit board plotter (LPKF ProtoMat S62) shown in Fig.11a. Subsequently, a thin PDMS layer was coated on the PCB by pouring degassed PDMS solution on top surface of PCB (Fig. 11b), flattening by a glass slide (Fig. 11c) and baking on a hot plate at 80 °C for 2 h. The PDMS solution was prepared by mixing two-part curing PDMS precursor solutions (A: B weight ratio = 10:1; Dow Corning, Midland, MI) and then degassing in a homemade chamber for 30 min under active vacuum (10^{-4} Torr). The glass slide used here was pre-silanized with (tridecafluoro1,1,2,2-tetrahydrooctyl)-1-trichlorosilane (T2492-KG, United Chemical Technologies, Levittown, PA) in the same chamber under the same vacuum condition for 30 min to obtain a hydrophobic surface. The thickness of the thin PDMS layer was determined by four 0.1 mm-high spacers placed on four corners of the PCB. After thermal curing, the flat thin PDMS layer was formed (Fig. 12d). The area of the circuit was pre-protected by scotch tap (Scotch Packaging Tape, 3M) during pouring PMDS precursor solution on PCB. After removing the scotch tap, two four-channel analog multiplexers (ADG607, Analog Devices) were soldered on the welding spots.

www.manaraa.com

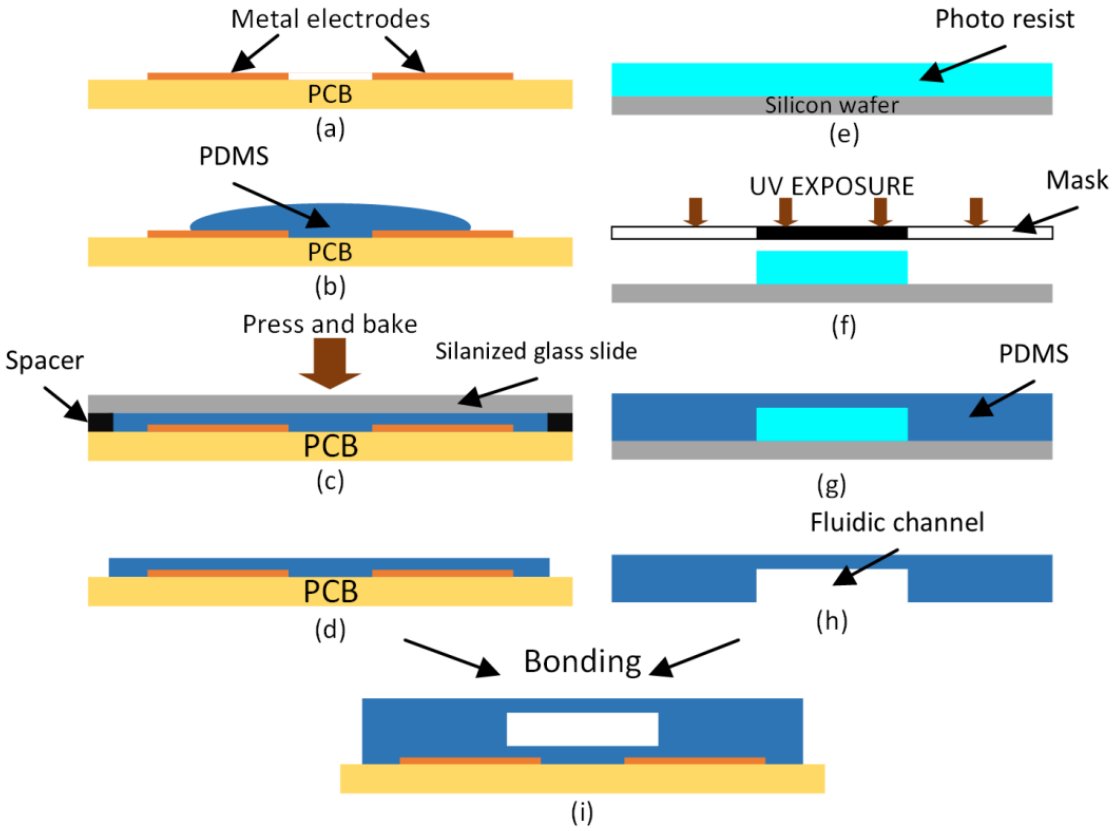

Figure 11: detailed device fabrication process flow. The steps include PDMS flatten, concentration gradient generator fabrication and PDMS bonding.

A master mold for 50 µm-deep liquid flow channels were made by spin-coating negative photoresist (SU-8-25, Microchem, Westborough, MA) on corresponding silicon wafers (Fig. 11e) and photopatterning them with high-resolution (10160 dpi) transparency film masks (Fig. 11f). The same degassed PDMS solution was then poured over the master molds in polystyrene petri dishes (Sigma-Aldrich, St. Louis, MO) and baked on a hot plate at 80 °C for 2 h (Fig. 11g). All necessary holes were created by punching through the channel layer at inlets and outlets. This PDMS channel layer was peeled off from the master mold by cutting off unwanted PDMS at the edges (Fig. 11h), and bonded on the PDMS side of PCB by oxygen plasma treatment (Fig. 11i). Careful alignment was needed in this step. Finally, the device was placed on a hotplate at 80 degrees Celsius for 1 h.

www.manaraa.com

Measurements, Results and Discussion

To validate the workability of the device in improving efficiency of electrical impedance measurement, we performed concentration measurements for ethanol, L-tartaric acid and L-malic acid involved during fermentation process for winemaking. During the fermentation of grape wine, the ethanol concentration increases from zero to ~12 % (v/v), while the sugar concentration drops to zero. The dominant organic acids in grape wine are L-tartaric acid and L-malic acid accounting for 70–90% of the total grape acidity. As the fermentation goes on, the L-tartaric acid remains relatively stable, while the L-malic acid is gradually converted into lactic acid and CO_2. The L-malic acid level is important for wine quality, because it not only affects the wine taste, but also may cause wine spoilage. Hence, the concentrations of ethanol, L-malic acid and L-tartaric acid are considered as the major criteria for wine quality evaluation and winemaking process monitoring[12].

The chosen samples have an equal concentration of L-tartaric acid of 5 g/L due to it is relatively stable percentage during the fermentation process. An L-tartaric acid (Sigma, 99.5%) and L-malic acid (Sigma, 99%) mixed solution was prepared by dissolving acid solids in distilled (DI) water with 10% and 4% w/w respectively, and loaded into a needle syringe (3mL, Safety-Lok). Two syringes loading with DI water, and one syringe loading with pure ethanol (Sigma, 99%) were prepared. The water syringes were connected to inlets a and d, the syringe with ethanol was connected to inlet b and the syringe with mixed acids solution was connected to inlet c. Each syringe was mounted on a digital syringe pump (780100, KD SCIENTIFIC). The initial infuse rate for four inlets were set as 0.072 µL/h, 0.028 µL/h, 0.2 µL/h and 0.1 µL/h respectively. After flowing 3 minutes to deliver a stable mixed solution to each outlet port, the device created concentration gradients shown in experiment #1 in table 1. After the impedances at eight outlets

www.manaraa.com

have been measured, the mixed acids solution was changed to 10% L-tartaric & 8% L-malic, 10% L-tartaric & 12% L-malic and 10% L-tartaric & 16% L-malic for experiments #2, #3 and #4 respectively, shown in table 1.

Table 1. Experiment #1 setup parameters for CGG and the output concentrations.

Exp-1					Exp-2				
	inlet	infusion rate	concentration			inlet	infusion rate	concentration	
input	a	0.072 uL/h	100% water		input	a	0.072 uL/h	100% water	
	b	0.28 uL/h	100% ethanol			b	0.28 uL/h	28% ethanol	
	c	0.2 uL/h	10% T 4%M			c	0.2 uL/h	10% T 8%M	
	d	0.1 uL/h	100% water			d	0.1 uL/h	100% water	
output	outlet	Ethanol %	T %	M %	output	outlet	Ethanol %	T %	M %
	0	14	5	2		0	14	5	4
	1	12	5	2		1	12	5	4
	2	10	5	2		2	10	5	4
	3	8	5	2		3	8	5	4
	4	6	5	2		4	6	5	4
	5	4	5	2		5	4	5	4
	6	2	5	2		6	2	5	4
	7	0	5	2		7	0	5	4
Exp-3					Exp-4				
	inlet	infusion rate	concentration			inlet	infusion rate	concentration	
input	a	0.072 uL/h	100% water		input	a	0.072 uL/h	100% water	
	b	0.28 uL/h	28% ethanol			b	0.28 uL/h	28% ethanol	
	c	0.2 uL/h	10% T 12%M			c	0.2 uL/h	10% T 16%M	
	d	0.1 uL/h	100% water			d	0.1 uL/h	100% water	
output	outlet	Ethanol %	T %	M %	output	outlet	Ethanol %	T %	M %
	0	14	5	6		0	14	5	8
	1	12	5	6		1	12	5	8
	2	10	5	6		2	10	5	8
	3	8	5	6		3	8	5	8
	4	6	5	6		4	6	5	8
	5	4	5	6		5	4	5	8
	6	2	5	6		6	2	5	8
	7	0	5	6		7	0	5	8

A precision LCR meter (Applent AT2817A) was connected to each IDE sensor through the addressing electronic circuit and a 100 mV AC voltage was applied to the sensing element. EIS was conducted by measuring the impedance response. Electrical impedances with real and

www.manaraa.com

imaginary parts from each sensor were scanned and recorded in 11 frequency points starting from 200 Hz and ending at 100 kHz. An average result from 10 measurements was adopted to improve the accuracy.

The dots in one curve of the Nyquist plot from right to left represent frequencies scanned from 200 Hz to 100 kHz. Compare impedance spectra curve between each sample at the same frequency within one figure, an increase of ethanol concentration leads to an increase of both real and imaginary parts of the impedance. Fig. 12b, c and d shows the Nyquist plot of measured impedances of eight samples with same 5% L-tartaric acid and a concentration gradient of ethanol from 0% to 14%, but different L-malic acid concentrations of 4%, 6% and 8% respectively. Compare impedance curves between Fig. 12a, b, c and d, an increase of L-malic acid concentration leads to an increase of imaginary part of the impedance. Since both ethanol and L-malic acid concentrations have influences on the impedance, PCA was adopted to simply the mapping relationship.

www.manaraa.com

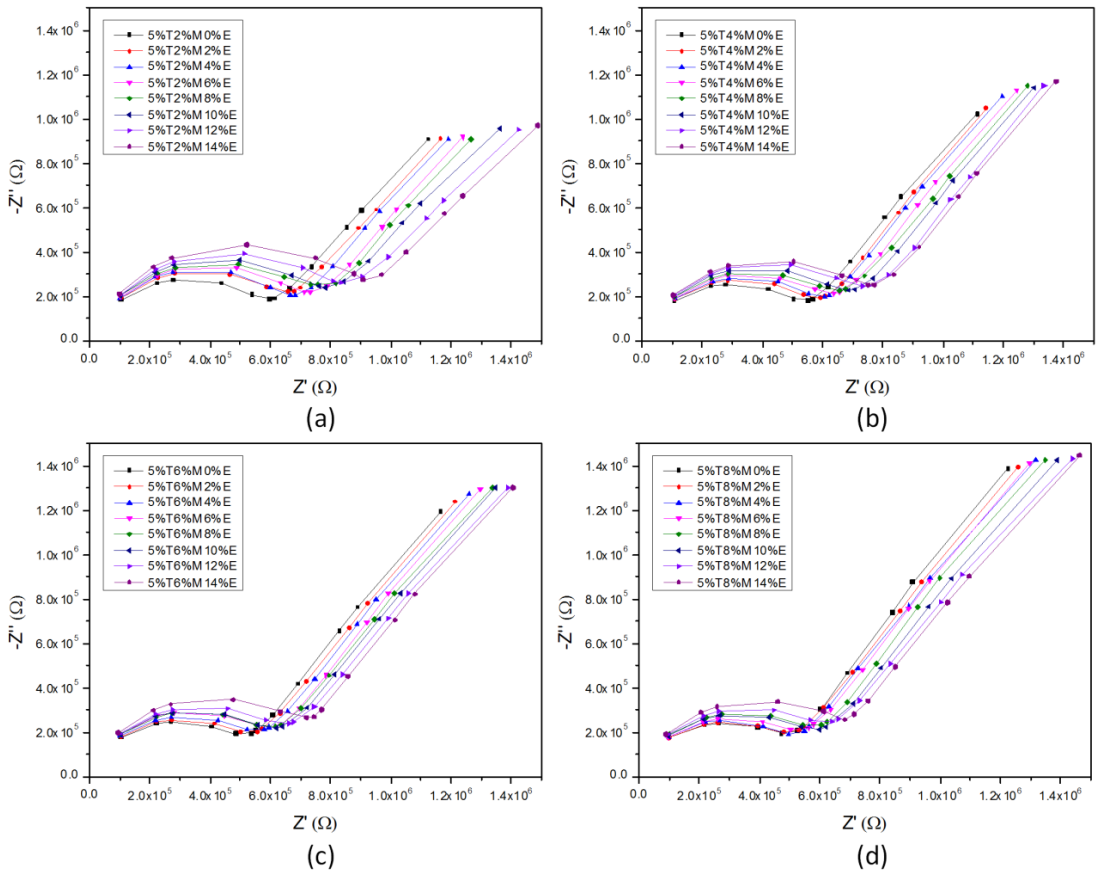

Figure 12: Nyquist Plot of electrical impedance parameters of (a) eight samples with constant concentrations of 5% L-tartaric acid and 2% L-malic acid and increasing ethanol concentration from 2% to 16%; (b) eight samples with constant concentrations of 5% L-tartaric acid and 4% L-malic acid and increasing ethanol concentration from 2% to 16%; (c) eight samples with constant concentrations of 5% L-tartaric acid and 6% L-malic acid and increasing ethanol concentration from 2% to 16%; (d) eight samples with constant concentrations of 5% L-tartaric acid and 8% L-malic acid and increasing ethanol concentration from 2% to 16%.

By analyzing the impedances for different solution mixtures utilizing PCA, the real and imaginary parts of impedances as a function of frequencies can be reduced to two principle components (PC1 and PC2). The variance of PC1 (84.2%) and PC2 (15.4%) is above 99% and therefore these components already contain significant information to represent the date in two dimensions. Clear separation between the clusters representing individual mixed samples with no overlap and a recognizable trend of concentration allows the identification of analytes. Group 5%T2%M shows the distributions of mixtures with 5% L-tartaric acid, 2% L-malic acid and an increasing of ethanol percentage from 2% to 16%. Group 5%T4%M shows the distributions of 5%

www.manaraa.com

L-tartaric acid, 4% L-malic acid; group 5%T6%M shows the distributions of 5% L-tartaric acid, 6% L-malic acid; group 5%T8%M shows the distributions of 5% L-tartaric acid, 8% L-malic acid all with ethanol percentage 2% to 16%. With an increase of ethanol concentration, PC1 increases; with an increase of L-malic acid concentration, PC2 decreases. Thus, the unknown concentrations combination of these three components in a mixture can be analyzed by measuring its electrical impedance with an impedance sensor and the use of PCA.

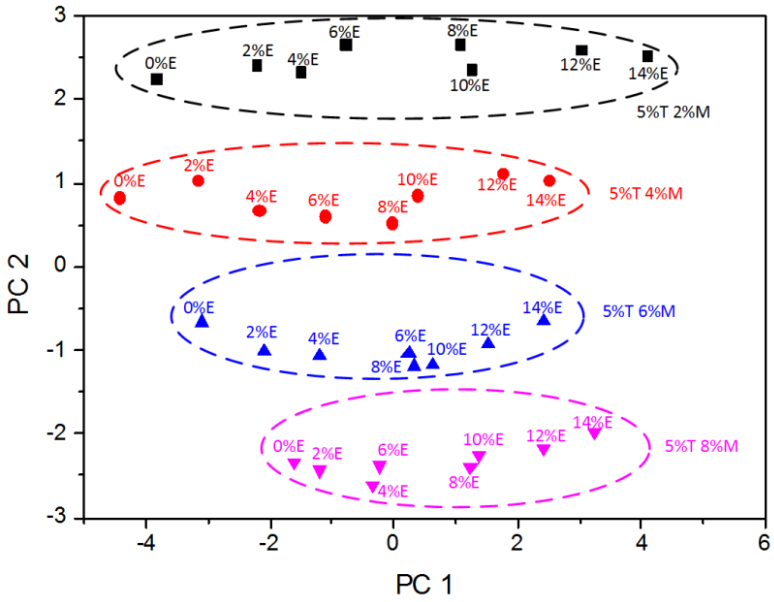

Figure 13: impedance analysis based on PCA with different acids and ethanol concentrations.

The data acquisition throughput can be further improved by scaling up the proposed microfluidic device. More mixer modules can be integrated into the CGG, a higher resolution of concentration gradient can be generated at outlets, where more IDE based sensors can be fabricated on the PCB. The estimation of generated concentration gradient of solutions at N outlets of CGG can be determined utilizing matlab with an iteration algorithm, which was used for the concentrations generation simulation at 8 outlets in section 2.1.

www.manaraa.com

Conclusion

A high-throughput microfluidic device for improved online measurement efficiency was demonstrated. The potential applications of the proposed microfluidic device are widespread since the electronic sensor based on electrical impedance measurement is one of the best choices for online, in-situ measurements of solution concentrations, which requires low cost, simple operation but sufficient data for mapping impedance to concentrations in solution. Future works includes scaling up this microfluidic device for higher accuracy and integrating the sensor into winemaking systems for online process control.

Acknowledgements

This work was supported in part by the Institute for Physical Research and Technology and the Plant Sciences Institute at the Iowa State University, and the U.S. National Science Foundation under Grants ECCS-1102354 and DBI-1353819.

References

[1] Wang, X. D., & Wolfbeis, O. S. (2012). Fiber-optic chemical sensors and biosensors (2008–2012). Analytical chemistry, 85(2), 487-508.

[2] Swinkels, D. W., Girelli, D., Laarakkers, C., Kroot, J., Campostrini, N., Kemna, E. H., & Tjalsma, H. (2008). Advances in quantitative hepcidin measurements by time-of-flight mass spectrometry. PLoS One, 3(7), 2706.

[3] Coffman, J. L., Kramarczyk, J. F., & Kelley, B. D. (2008). High-throughput screening of chromatographic separations: I. Method development and column modeling. Biotechnology and bioengineering, 100(4), 605-618.

[4] Y. Zhao, B. Zhang, Y. Liao, Experimental research and analysis of salinity measurement based on optical techniques, Sens. Actuators B 92 (2003) 331–336.

[5] R. Xu, Z. Lv,Y.G. Zhang, G. Somesfalean, Z.G. Zhang, Concentration evaluation method using broadband absorption spectroscopy for sulfur dioxide monitoring, Appl. Phys. Lett.

[6] A. Abdelghani, N. Jaffrezic-Renault, SPR fiber sensor sensitised by fluorosiloxane polymers, Sens. Actuators B 74 (2001) 117–123.

www.manaraa.com

[7] Suni, I. I. (2008). Impedance methods for electrochemical sensors using nanomaterials. TrAC Trends in Analytical Chemistry, 27(7), 604-611.

[8] Pejcic, B., & De Marco, R. (2006). Impedance spectroscopy: Over 35 years of electrochemical sensor optimization. Electrochimica Acta, 51(28), 6217-6229.

[9] F. Lisdat and D. Schäfer, "The use of electrochemical impedance spectroscopy for biosensing", Anal Bioanal Chem 10, 2008.

[10] Zöpfl, A., Lemberger, M. M., König, M., Ruhl, G., Matysik, F. M., & Hirsch, T. (2014). Reduced graphene oxide and graphene composite materials for improved gas sensing at low temperature. Faraday Discuss., 173, 403-414.

[11] Eslamimanesh, A., Gharagheizi, F., Mohammadi, A. H., & Richon, D. (2011). Artificial neural network modeling of solubility of supercritical carbon dioxide in 24 commonly used ionic liquids. Chemical engineering science, 66(13), 3039-3044.

[12] Rana, S., Page, R. H., & McNeil, C. J. (2011). Impedance spectra analysis to characterize interdigitated electrodes as electrochemical sensors.Electrochimica Acta, 56(24), 8559-8563.

[13] Dertinger, S. K., Chiu, D. T., Jeon, N. L., & Whitesides, G. M. (2001). Generation of gradients having complex shapes using microfluidic networks.Analytical Chemistry, 73(6), 1240-1246.

[14] Noo Li Jeon, Stephan K. W. Dertinger, Daniel T. Chiu, Insung S. Choi, Abraham D. Stroock, andGeorge M. Whitesides. Generation of Solution and Surface Gradients Using Microfluidic Systems. Langmuir, 2000, 16 (22), pp 8311–8316.

[15] Sicong Zheng, Qiang Fang, Irena Cosic. An investigation on dielectric properties of major constituents of grape must using electrochemical impedance spectroscopy. Eur Food Res Technol (2009) 229:887–897.

[16] Stephan K. W. Dertinger, Daniel T. Chiu, Noo Li Jeon, and George M. Whitesides. Generation of Gradients Having Complex Shapes Using Microfluidic Networks. Anal. Chem., 2001, 73 (6), pp 1240–1246.

www.manaraa.com

CHAPTER 4. MINIATURIZED CONTINUOUS-FLOW WINERY

Modified from a provisional patent application submitted to The United States Patent and Trademark Office

Daniel Attinger,[1] Liang Dong,[2] and Yuncong Chen[2]

[1]Department of Electrical and Computer Engineering, Iowa State University, Ames, Iowa 50011, USA

[2]Department of Mechanical Engineering, Iowa State University, Ames, Iowa 50011, USA

Field of the Invention

The invention relates generally to wine-making. More particularly, but not exclusively, the invention is directed towards a miniaturized wine making apparatus, system, and method that allows for rapidly screening for the best qualities of the parameters involved in making wine.

Background of the Invention

Wine is typically produced in large batches, with volumes typically in the range of 10-100,000L. Grape juice is mixed with yeast, which consumes the sugars in the juice. Carbon dioxide and alcohol is released during the consumption of the sugar by the yeast, fermenting the juice to create the wine. Alcoholic fermentation occurs within one to two weeks, and the remaining winemaking operations occur within weeks to months. Yeast cells are dispersed in the juice. Monitoring of fermentation and production is done by sampling.

Because of the traditional method of making wine, testing is slow and cumbersome. Sometimes, an entire batch of wine can be ruined.

www.manaraa.com

Furthermore, because of the slow and lengthy process of traditional batch-style winemaking, there is little chance to adjust the variables, such as type and amount of yeast and grape combination, temperature of fermentation, amount of light, as well as other factors that could affect the taste, alcohol content, and other factors that determine the quality of wine produced. Climate and maturation differences vary from year to year, which makes it difficult to evaluate the effect of modifications in the winemaking process. Quality improvements in winemaking occur by incremental modifications, usually once a year.

Therefore, there is a need in the art for a quick and simple method of screening the variables of winemaking in an easier fashion to determine the best combinations for creating higher qualities of wine.

Brief Summary of the Invention

Therefore, it is a primary object, feature, and/or advantage of the invention to improve on and/or overcome the deficiencies in the art.

It is another object, feature, and/or advantage of the invention to provide a miniaturized continuous-flow winery.

It is yet another object, feature, and/or advantage of the invention to provide a winemaking process with reduced alcoholic fermentation time.

It is still another object, feature, and/or advantage of the invention to provide a winemaking apparatus, system, and method that provides for greater control of gradients of the winemaking conditions.

It is a further object, feature, and/or advantage of the invention to control the type of yeast and temperature of the process to produce near infinite combinations of variables for producing wine.

www.manaraa.com

It is yet a further object, feature, and/or advantage of the invention to aid in improving large-scale winemaking processes in ever-changing climate conditions.

It is still a further object, feature, and/or advantage of the invention to provide an apparatus, system, and/or process that could be used to produce generally any fermented beverage.

These and/or other objects, features, and advantages of the invention will be apparent to those skilled in the art. The invention is not to be limited to or by these objects, features and advantages. No single embodiment need provide each and every object, feature, or advantage.

According to some aspects of the invention, a miniaturized, continuous-flow beverage fermenting apparatus, system, and method is provided that includes immobilized yeast cells, mass transport via porous membranes, inline alcohol sensing, and temperature control. The components could be used with grape juice, for example, to produce wine. However, other fermented beverages are also contemplated to be produced with the invention.

It is contemplated that the system be used to rapidly screen for the best quality of fermented beverage, such as by adjusting the parameters involved with making the fermented beverage, which could include, but is not limited to, yeast types and fermentation temperature.

www.manaraa.com

Brief Description of the Drawings

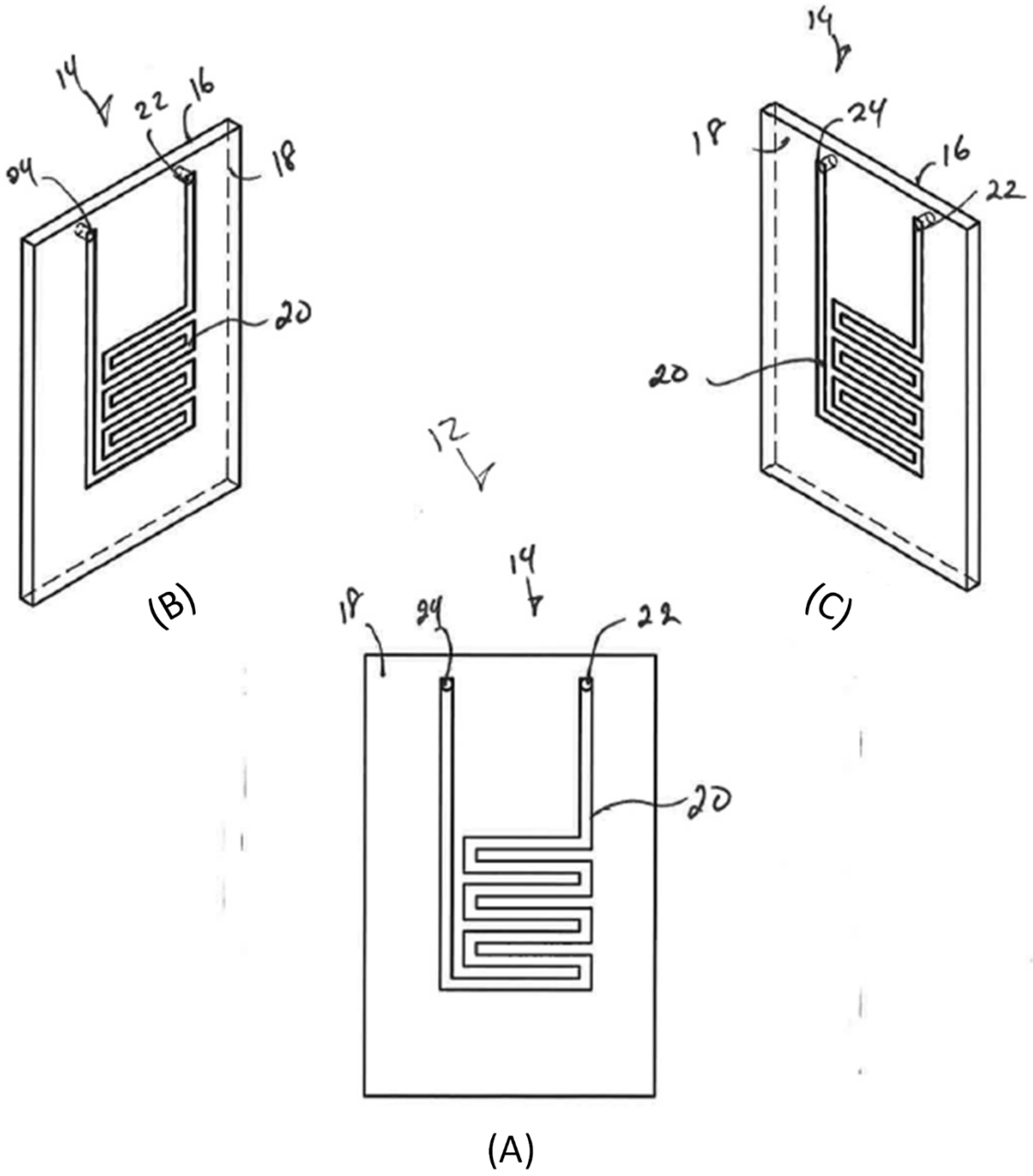

Figures 14: (A)-(C) Views of a first plate for use with a beverage fermenting system according to aspects of the invention.

www.manaraa.com

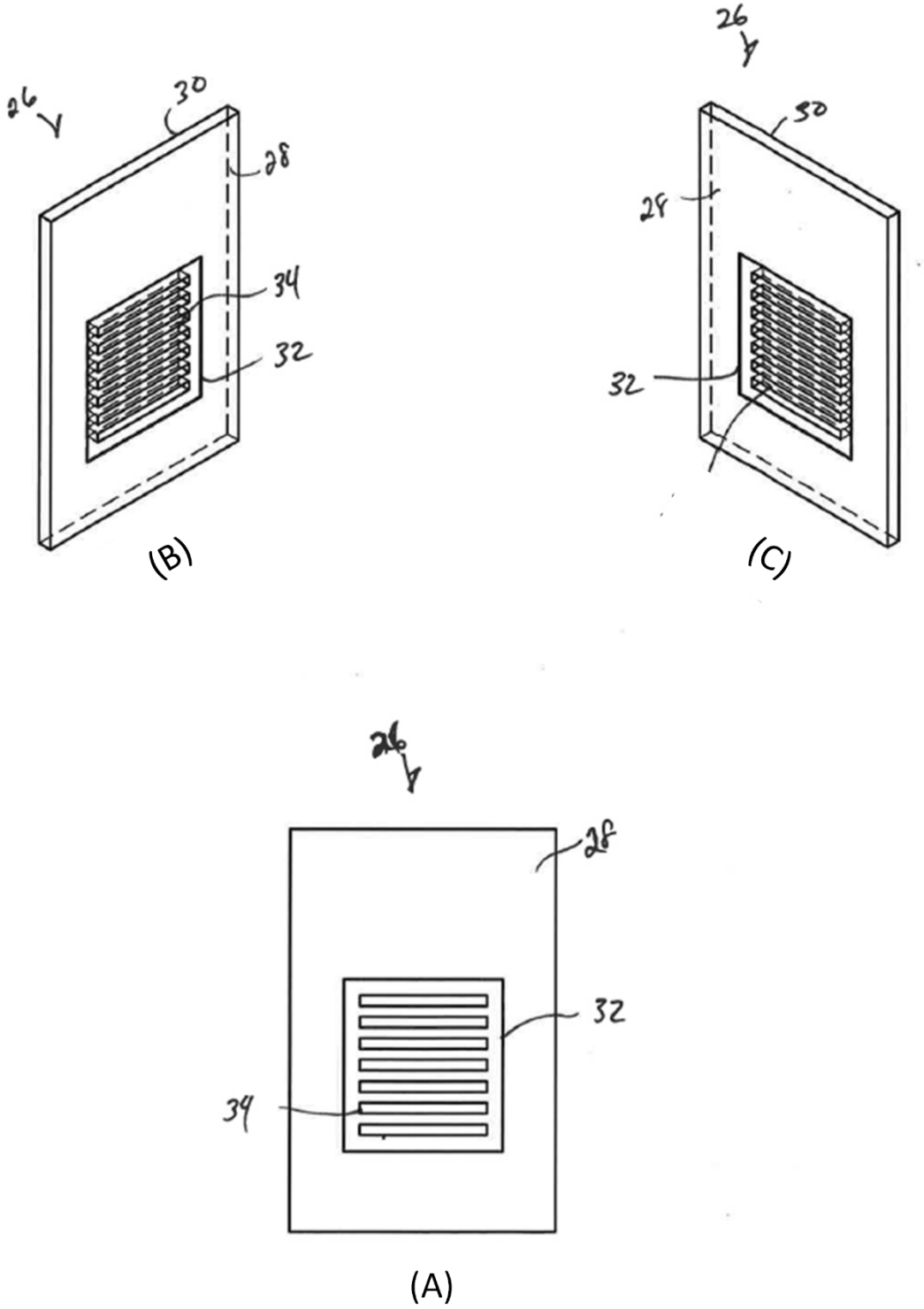

Figures 15: (A)-(C) Views of a second plate for use with a beverage fermenting system according to aspects of the invention.

www.manaraa.com

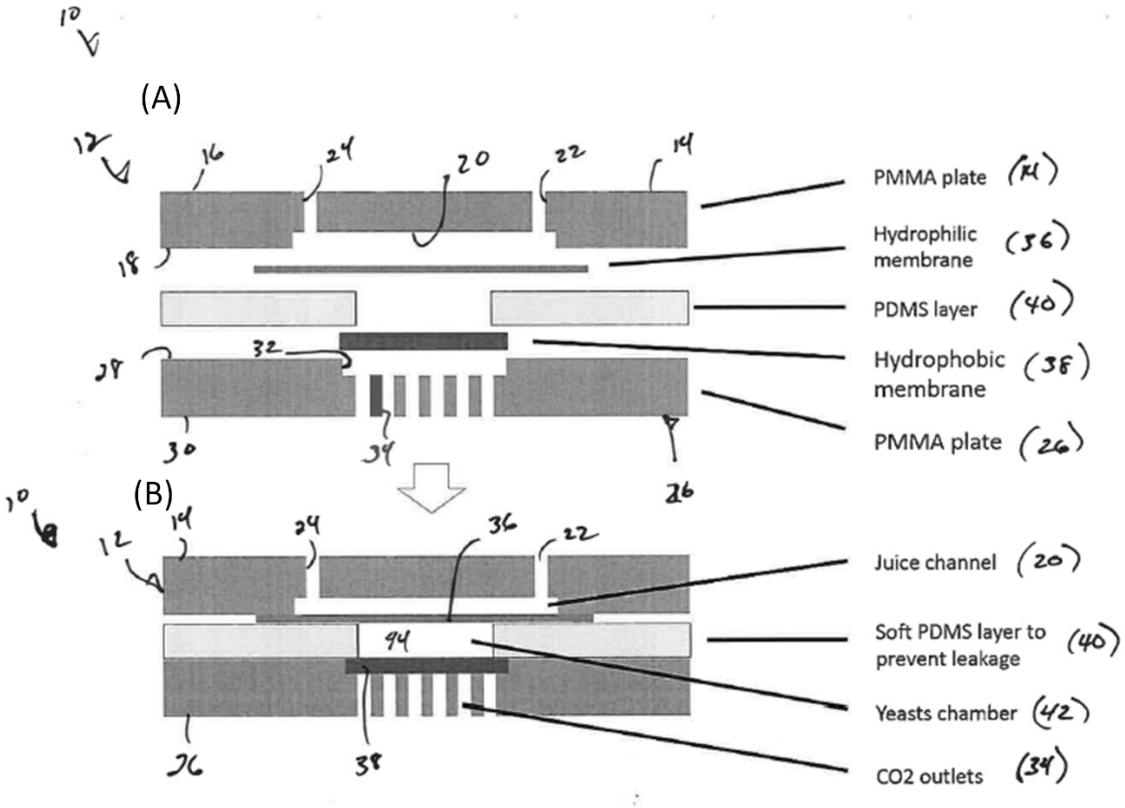

Figure 16: (A)-(B) Schematics of a beverage fermenting apparatus and system according to aspects of the invention.

www.manaraa.com

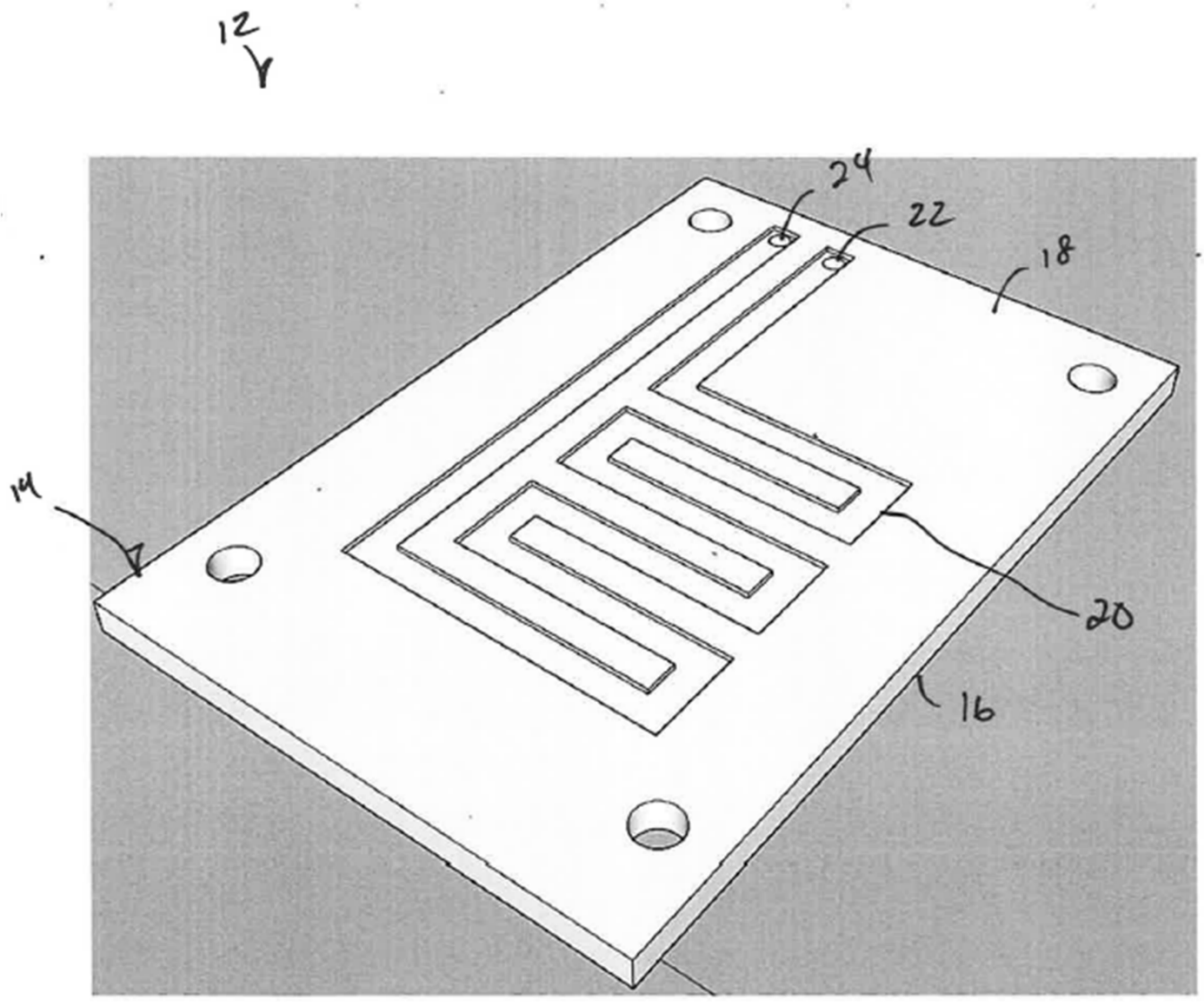

Figure 17: A perspective view of a first plate for use with a beverage fermenting system according to aspects of the invention.

www.manaraa.com

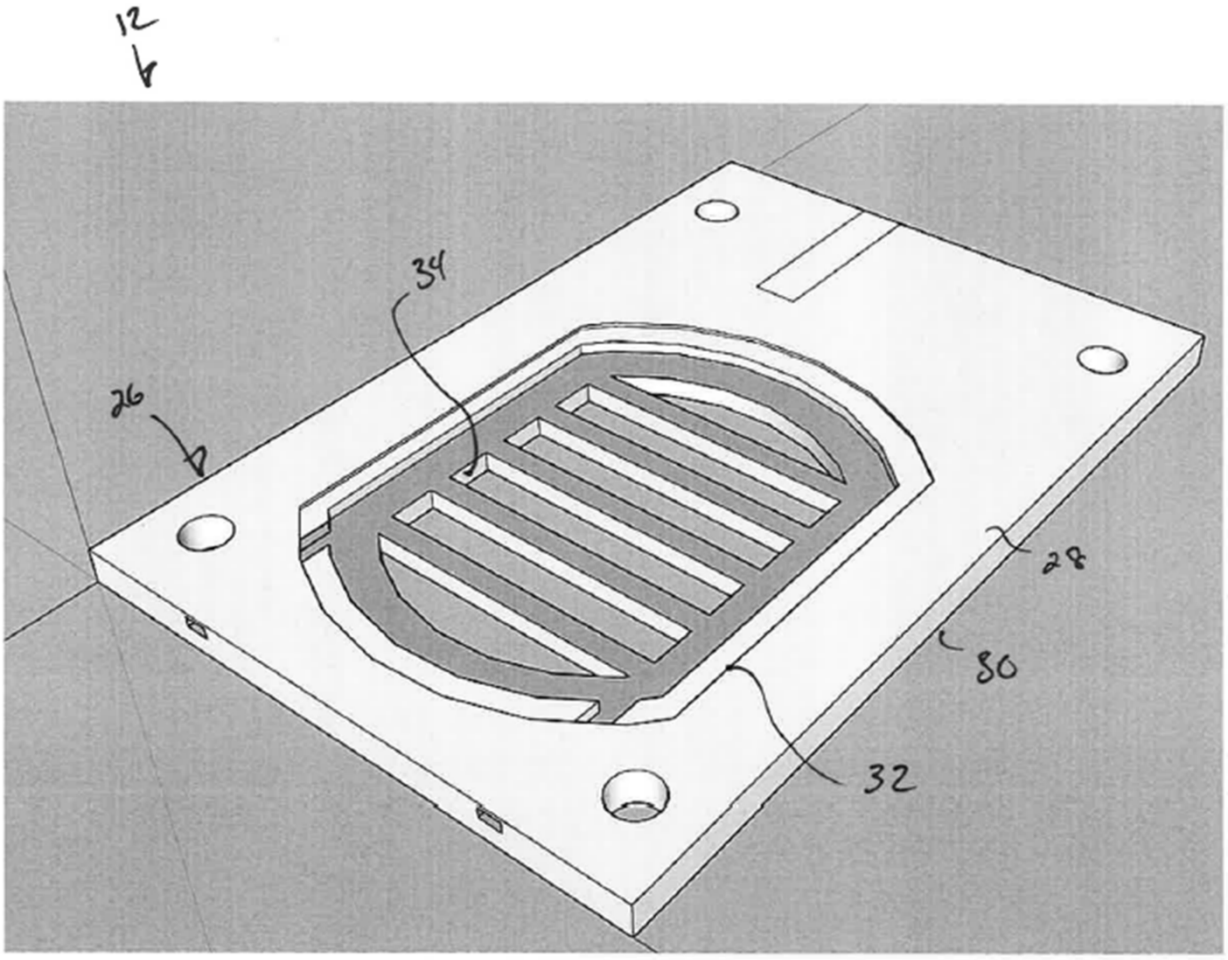

Figure 18: A perspective view of a second plate for use with a beverage fermenting system according to aspects of the invention.

www.manaraa.com

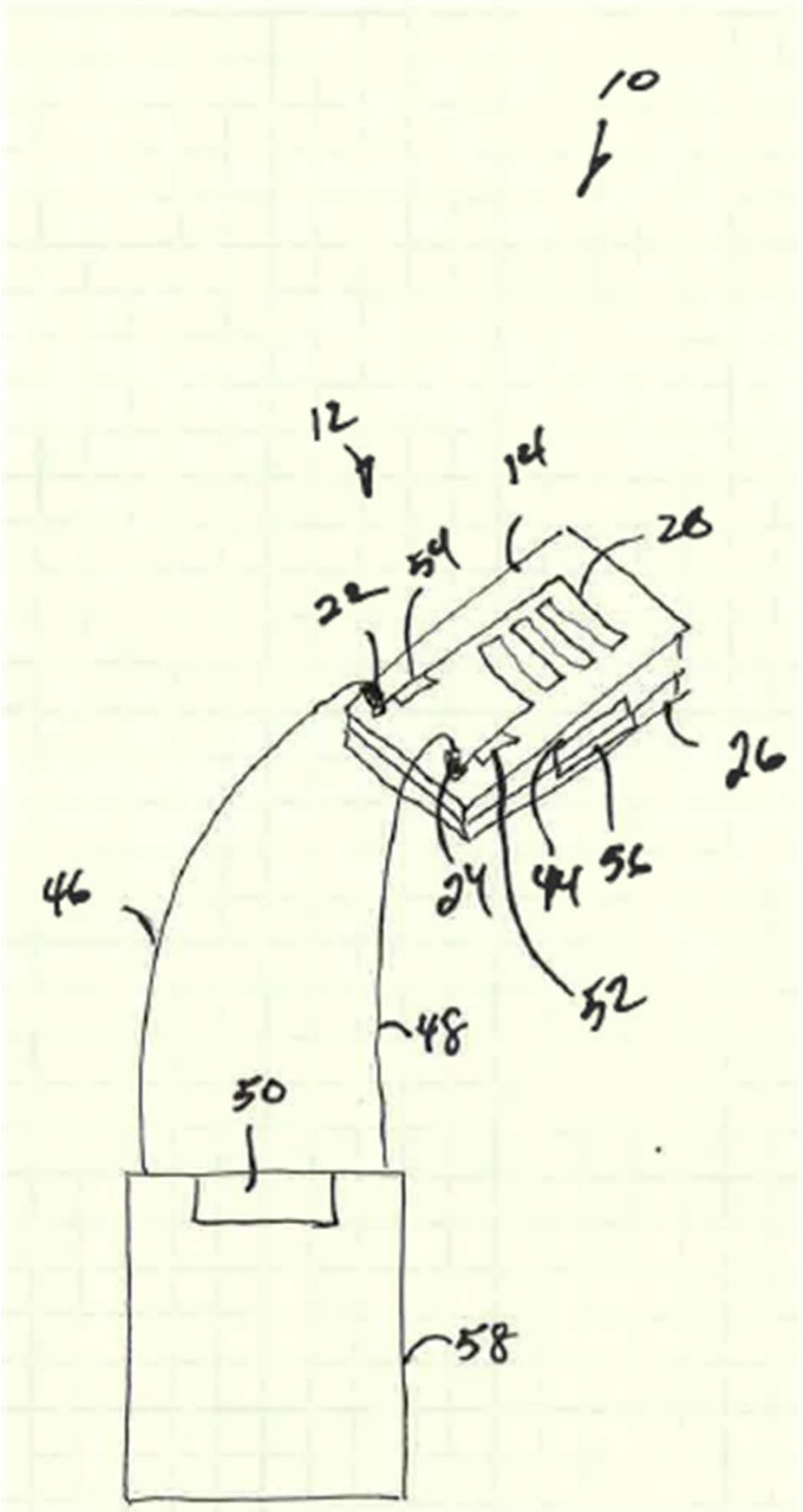

Figure 19: A sketch of a beverage fermenting system according to aspects of the invention.

www.manaraa.com

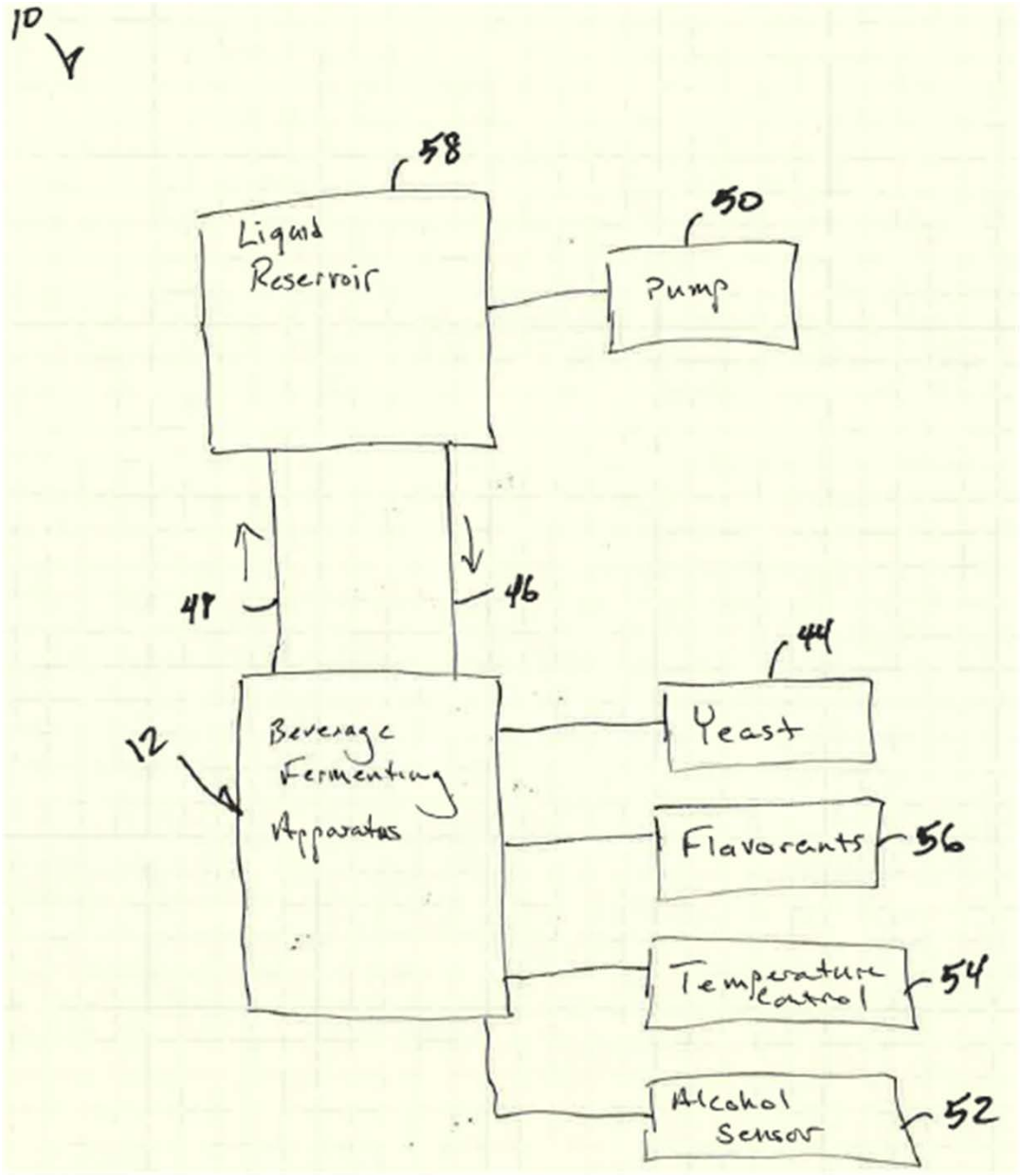

Figure 20: A block diagram showing components of a beverage fermenting system.

Various embodiments of the invention will be described in detail with reference to the drawings, wherein like reference numerals represent like parts throughout the several views. Reference to various embodiments does not limit the scope of the invention. Figures represented herein are not limitations to the various embodiments according to the invention and are presented for exemplary illustration of the invention.

www.manaraa.com

Detailed Description of the Invention

The invention is for a beverage fermenting system 10, which utilizes a continuous flow rather than batch approach for the fermentation of a beverage, such as a fermentation of grape juice to make wine. This is done on a miniaturized or very small scale, such as wherein the volume produced by the system may be on the order of 1ml per unit. The alcoholic fermentation can occur within one to three days, as opposed to one to two weeks, which is required for large batch alcoholic fermentation. To accomplish such, and as will be understood, the yeast is not dispersed in the liquid, such as grape juice, but is separated from the liquid by a porous hydrophilic membrane, and from the ambient air by hydrophobic membrane. In-line electrical impedance sensing monitors the alcohol content of the liquid as it is circulated through the system. An alcohol sensor and/or temperature control can be integrated with the system as well to monitor the system and to control the variable of temperature during the fermenting process. For example, the temperature could be controlled via integrated thermoelectric planar elements. As will be understood, the miniaturized, continuous flow system provided by the present disclosure will allow for greater variability in the factors that go into the fermentation of a liquid, such as yeast type, flavorings, temperature, humidity and/or some combinations thereof, to allow for greater flexibility and testing to be able to create potentially new types of fermented beverages based on the alterations of the input variables. However, it is believed that the invention will allow quick and easy testing to screen two critical winemaking parameters, the yeast type and the operating temperature.

The invention can both improve the quality of fermented beverages, such as wines, by testing different variations of inputs, and can also provide for future planning in beverage production. For example, as the earth's climate is changing, this could affect the fermentation and

www.manaraa.com

qualities of fermented beverages created using traditional systems and methods. The beverage fermenting system 10 of the invention will help develop and adapt these processes to changing climates, such as by testing different types of yeast and other variables at different climates, such as higher temperatures. The long term outcome is envisioned to be a more robust and vibrant fermented culture, even assuming some of the changes in climate.

Therefore, the figures show exemplary aspects of the invention, which provide for providing an apparatus, system, and/or method for fermenting a beverage in a miniaturized fashion such that a small scale amount of fermented beverage can be produced with generally infinite variability. Such a system is shown in full in Figure 19. As shown in Figure 19, the beverage fermenting system 10 includes the components of a housing 12, which may also be known as a chip or plated housing. The housing 12 includes a first plate 14 and a second plate 26 in matingly engagement. A liquid reservoir 58 contains and amount of liquid, such as grape juice to store therein. The grape juice stored in the reservoir 58 can be pumped, such as by hydrostatic pump 50 through an inlet tube 46 and towards the chip 12. The juice enters an inlet 22 in a first plate 14, where it is passed through a channel 20. The channel 20 passes the juice adjacent an amount of yeast, such as a paste or cartridge and continued out the chip 12 via the exit 24. The juice is then circulated back to the reservoir 58 via the exit tube 48. The continuous circulation of the juice from the reservoir 58 to and from the chip 12 will allow the sugars of the juice to be consumed by the yeast in the chip 12. This interaction will cause the reaction of alcohol being formed within the juice, and carbon dioxide to be omitted from the reaction. The carbon dioxide can be omitted from the second plate 26, such as via the exhaust ports 34. A membrane can separate the yeast from the exhaust ports to prevent any liquid from escaping the chip 12. Therefore, the alcohol will continue to build within the juice as it is circulated between the reservoir 58 and the chip 12 until

www.manaraa.com

alcohol sensors 52 within the path can detect, such as by electrical impedance, that the alcohol content has reached a desired level. The liquid can then be removed from the system and sent for testing of beverage quality.

The components of the system are shown generally in Figures 14-19. Figures 14A-14C show various views of a first plate 14 of the housing 12 of the beverage fermenting system 10. The plate 14 shown in Figures 14A-14C is generally planar member in the shape of a rectangle. While a rectangular shape is shown, it should be appreciated that this is not the only shape, and generally any shaped could be utilized for the chip. It should be further appreciated that the thickness of the plate 14 is minimal to reduce the overall thickness of the chip housing 12.

Further components of the first plate 14 include a channel 20, which is formed into an interior 18 side of the plate 14. The interior side 18 is generally opposite the exterior side 16, with both sides being substantially planar. The channel 20 can be formed by machining, molding, or other process to create a recessed channel into one of the interior or exterior sides of the plate 14. However, as the first and second plates will be mating engagement, it is ideal to position the channel on the interior side of the plate 14. The channel 20 as shown in the figures starts at an inlet aperture 22 and ends at an exit aperture 24. The inlet and exit apertures 22, 24 are apertures generally through the entire thickness of the plate 14. However, as has been disclosed, the recessed channel 20 will not extend the full distance between the interior 18 and the exterior 16 of the plate, and instead will only extend a short distance. Furthermore, the channel 20 as shown in the figures is shown to include a generally serpentine portion wherein the channel goes in a back and forth manner. This back and forth and/or serpentine configuration of the channel 20 will allow the juice or other liquid flowing through the channel 20 to pass adjacent an amount of yeast in such a manner that a high surface area of the yeast will be passed by the juice, thus increasing the amount of time

www.manaraa.com

in contact with the yeast. This will decrease the time it takes to ferment the juice by the yeast. However, it should be appreciated that while the back and forth serpentine configuration of channel 20 is utilized, this is not to be considered the only configuration that can be taken by the channel 20. For example, a circular shape, squared shape, spiral shape, or generally any other configuration which can increase the surface area and/or surface time in which the juice will pass via the yeast is to be contemplated as part of the present disclosure.

Figures 15A-15C show some aspects of an embodiment of a second plate 26, which can be used with the first plate 14 to form the chip housing 12. The second plate 26 takes generally the same form and/or shape of the first plate 14. Therefore, while the plates are shown as rectangular-shaped in the figures, this is not to be construed as limiting on the invention. However, for purposes of disclosure, the second plate being rectangular-shaped will be described. The plate 26 includes an interior side 28 and an exterior side 30. A recessed portion 32 is formed on the interior side 28 of the second plate 26. At the recessed portion 32 and extending from the interior side 28 to the exterior side 30 are a plurality of exhausts apertures or outlets 34. As will be understood, the exhaust apertures 34 will allow the carbon dioxide created by the reaction of the yeast and the sugars in the fermenting liquid to escape during the fermenting process. Therefore, the number, shape, and other properties of the exhaust outlets need not to be limited to that specifically shown in the figures, and can take generally any shape, size, and/or number.

Furthermore, it is contemplated that the first and second plates 14, 26 comprise a polymer material. The polymer material, such as PMMA, will provide rigidity, will also allow for flexibility in the design of the channels, outlets and other components of the plates. Furthermore, it should be appreciated that the recessed portion 32 of the second plate 26 would be generally aligned with the serpentine portion of the channel 20 as is shown in the figures. This will provide

www.manaraa.com

a region where the yeast can be positioned, as will be understood. Therefore, as the yeast is positioned generally in the recessed portion 32 of the second plate 26, the juice or other liquid passing through the channel in the serpentine portion will have the greatest amount of time interacting with the yeast at the recessed portion 32, wherein the fermentation time as the liquid circulates will be greatly reduced, which will produce a fermented liquid in the shortest amount of time possible. Having the outlets at generally the same location as the recessed portion 32 and the serpentine portion of the channels 20 will also provide the benefit of allowing the direct exhaust of the carbon dioxide created by the interaction between the yeast and the fermenting liquid.

Figures 16A and 16B show additional components of the beverage fermenting system 10 including the components of the housing or chip 12. For example, Figure 16A is a generally exploded and sectional view from an end of the housing 12 to show additional internal components thereof. As is shown, the first plate 14 is provided with the channel 20 on the interior 18, and the inlet and outlet 22, 24 apertures positioned from one side to the other. Positioned adjacent the interior 18 of the first plate 14 is a hydrophilic membrane 36. The hydrophilic membrane 36 is a water loving membrane that will pull the liquid travelling through the channel 20 towards the membrane. As will be understood, this will pull the juice towards the yeast stored in a yeast chamber 22, to increase the interaction between the juice and the yeast in order to decrease the fermentation time. The physical barrier between the yeast and the juice/wine facilitates the separation of the yeast from the wine, which is typically done in large scale wineries by sedimentation and racking. This allows for the easy sequential use of different yeasts during the same fermentation, without the need to wait -for weeks- for sedimentation to occur.

A PDMS layer 40 can be positioned generally around the recessed portion 32 of the second plate 26, which can aid in sealing the chip 12 when the first plate 14 and second plate 26 are

www.manaraa.com

positioned in connection or meeting with another such as shown in Figure 16B. The layer will be outside the fermenting components of the system such that it will not affect the fermentation thereof, but it will instead seal the housing to prevent any leakage thereof.

A yeast chamber 42 is positioned adjacent the opposite side of the hydrophilic membrane 36. As has been disclosed, a yeast can be positioned within the yeast chamber 42. The yeast can be inserted such as by smearing a yeast on the backside of the hydrophilic membrane 36 or can be inserted via a cartridge or other member. Such a configuration utilizing a cartridge will allow for a quick and easy switching of yeast for a particular chip set to allow for greater variability and fermenting the liquid circulating through the system. The modularity of the yeast will allow for quick and easy variability to allow for different types of yeast to interact with the liquid to determine which yeast and liquid combination will provide the highest quality of fermented beverage for varying inputs, such as temperature, humidity and the like. Positioned on an opposite side of the yeast chamber 42 is a hydrophobic membrane 38. Hydrophobic materials are generally water repelling such that it will repel any liquid coming near it. However, the hydrophobic membrane is gas permeable to allow gases to pass therethrough. Therefore, the hydrophobic membrane will ensure that any juice or other liquid that could potentially pass through the hydrophilic membrane will be repelled back towards said hydrophilic membrane by the hydrophobic membrane to mitigate the possibility that the liquid will be passed out the exhaust ports 34 of the second plate 26. However, as the hydrophobic membrane 38 is gas permeable, the carbon dioxide gases created by the reaction of the yeast consuming the sugars in the fermenting liquid will be allowed to pass out, such as in the direction of the arrow shown in Figure 16A. As is shown in Figures 16A and 16B, the hydrophobic membrane 38 can be positioned generally in the recessed portion 32 on the interior 28 of the second plate 26 such that it will be seated within

www.manaraa.com

the area in and around the exhaust ports 34 such that any fermented liquid will be repelled away from said exhaust apertures 34.

Figure 16B shows a sectional view of a chip 12 in which the components are in mating engagement with one another. Therefore, the inlet and outlet ports 22, 24 are shown in communication with the juice channel 20, which is on an upper side of the hydrophilic membrane 36. Therefore, it can be understood that the juice will enter the inlet port 22 and be passed through the channel 20 on the upper side of the hydrophilic membrane 36 until it reaches the exit aperture 24 where it will pass back towards the liquid reservoir. The yeast chamber 42 can be filled with a yeast 44, such as by a cartridge, smear, or otherwise. The yeast chamber is a chamber generally between a bottom side of the hydrophilic membrane 36 and an upper side of the hydrophobic membrane 38 to create a chamber. Surrounding said chamber and between the outer perimeters of the first plate 14 and the second plate 26 can be a PDMS layer, which can prevent leakage of the system. As mentioned, the hydrophobic membrane 38 can be positioned in a recessed portion 32 of the interior 28 of the second plate 26. This recessed portion can include a plurality of outlet or exhaust ports 34, whereas carbon dioxide can be released through the hydrophobic membrane and out the chip 12.

Figures 17 and 18 show additional aspects of the chip housing 12. For example, Figure 17 shows another embodiment of a first plate 14, wherein a different shaped channel 20 is included. However, the general principles of the previous system will be intact wherein the juice or other liquid will enter an inlet port 22, will pass in a serpentined manner through the channel 20 and will exit the outlet port 24 back towards the liquid reservoir. In addition, the channel 20 will be positioned generally on the interior side 18 of the plate 14.

www.manaraa.com

Figure 18 is an exemplary embodiment of another version of the second plate 26 of the housing 12. As shown in Figure 18, the interior 28 of the plate will include a recessed portion 32 which will terminate at a plurality of exhaust ports 34. As mentioned, the recessed portion 32 will create a flange portion around the outlet section 34, wherein the hydrophobic membrane can rest on the flange portion of the recessed 32 on the interior 28 of the second plate 26.

Figure 19 is an exemplary embodiment of a beverage fermenting system 10, as previously disclosed. For example, Figure 19 shows the chip 12 in connection with a liquid reservoir 58. The liquid reservoir 58 contains an amount of liquid to be fermented, such as grape juice. A pump 50, such as a hydrostatic pump, can be operatively connected between the reservoir 58 in an inlet and exit tube 46, 48 which extend between the reservoir 58 and the chip 12. Therefore, the pump can be operated to circulate the liquid between the reservoir 58 and the chip 12 until such time as the liquid has fermented to a predetermined alcohol content. The alcohol content can be tested via electrical impedance monitoring, such as at the location shown by the numeral 52 in Figure 19. Such a location is provided near the outlet 24 of the first plate 14. Therefore, the fermenting liquid has had a chance to pass through the serpentine channel 20 adjacent the yeast to allow the yeast to consume the sugars in the liquid. Such as reaction produces both carbon dioxide and alcohol, wherein the alcohol is remained in the juice. The alcoholic content will affect the electrical impedance of the liquid as it ferments, wherein the content can be determined on the impedance. Therefore, having a sensor 52 after the liquid has passed the yeast and before it exits the chip 12 will allow the best location for testing said alcohol content. The circulation can continue until such alcoholic content has reached a predetermined or chosen amount, such as based upon the type of fermenting beverage being produced by the system 10.

www.manaraa.com

Further components shown in Figure 19 include a temperature control 54, which can adjust the temperature of the liquid as it passes through the chip 12. The control of the temperature will allow for different combinations of yeast and temperature of the liquid to be tested to determine the best condition for creating the highest quality of fermented beverages based on inputs such as temperature and yeast type. As mentioned, temperatures are controlled via thermoelectric planar elements, and can be changed within seconds. In a traditional winemaking, this takes days. Further sensors and/or controls could include humidity controls to affect the humidity of the chip itself, as well as movement controls such as haptic controls. Such controls could attempt to mimic real life fermenting conditions based on different locations around the world to determine the best combinations of temperature, type of fermenting liquid, and/or yeast to produce the highest quality of fermented beverage based on said variable inputs. Therefore, it is also contemplated that different yeasts 44 could be included with the system. The yeast could be modular such that they are included on cartridges or other transport members, which can be easily inserted or applied in the system such that they could be swapped out with relative ease. Such cartridges could be slid into a slot between the first and second plates 14, 26 of the chip 12 to allow for switching out of these types. Additional cartridges could include flavorings 56, which could also be modular to allow for greater variability of the fermenting process.

Figure 20 shows a block diagram of the system, which can be explained in the process as follows. A fermenting liquid, such as a grape juice or other liquid can be stored in a liquid reservoir 58. A pump 50 such as a hydrostatic pump, can be operatively connected to the reservoir 58 as well as an inlet tube 46 and an exit tube 48, which extend between the liquid reservoir and the beverage fermenting apparatus 12, which is also known as the chip. The pump is operated to circulate the liquid from the reservoir 58 to and from the beverage fermenting apparatus 12. While

www.manaraa.com

at the apparatus 12, the juice will pass through a channel 20 as previously disclosed. The channel 20, which is separated from yeast 44 via a hydrophilic membrane 36, will allow the juice to interact with the yeast while being separated therefrom. However, as the channel is shaped and configured to allow the juice the greatest amount of time or interaction with the yeast, the amount of time for the fermentation to occur will be at a minimal. The interaction between the juice and the yeast will create both alcohol and carbon dioxide. A hydrophobic material on the opposite side the yeast will drive the alcohol towards the juice, while allowing the carbon dioxide to pass out the beverage fermenting apparatus 12, such as the outlet ports 34. The system is continued until it has been determined, such as by an alcohol sensor 52, that the juice circulated through the system has reached the desired alcohol content for the type of beverage being fermented. At this time, the fermented liquid can be tested for quality to determine whether the inputs used produced a high enough quality of fermented beverage for consumption.

Additional components as shown in Figure 20 include a temperature control 54 and flavorings 56, which are associated with the beverage fermenting apparatus 12. For example, the temperature control 54 can adjust the temperature of the juice or other liquid as it passes through the system. This will allow testing of the fermenting process at a variety of temperatures to determine the ideal temperature to create a high quality fermented beverage based on the combination of yeast and liquid. The flavorings 56, which could be modular in nature, could be added to produce additional flavors for the fermented beverage, as may be desired for a particular fermented beverage.

Therefore, a miniaturized, continuous flow beverage fermenting apparatus and system has been shown and described. It is contemplated that the miniaturization of the system will allow for a great number of advantages. For example, the volume of fermented liquid produced by such as

www.manaraa.com

system is contemplated to be on the scale of 1-4ml. This volume can be fermented in a quick manner, e.g., as short as a day. Thus, the testing can be done in a day based on the different variable inputs for fermenting the beverage to determine the best combination of inputs for creating a large scale or large batch of the same fermented beverage. In addition, mass transport is faster because it is based on diffusion over small lengths scales rather than confection diffusion. The small scale and quickness of the fermentation can allow for a greater number of recipes to be used at a single time which cannot be done in large batch fermenting, as it is now utilized. Therefore, there is more flexibility in/or experimentation with the fermenting process to determine the best recipe. In addition, the concise and fast control of the temperatures of the fermenting process can be achieved which allow for greater flexibility in both changing climates, as well as determining an ideal temperature for fermenting a liquid. For example, it is known that certain beverages such as wine, are fermented at optimum temperatures. However, due to the changing climates around the world, this may not be as easily accomplished. Therefore, by utilizing a different yeast in combination with a different grape juice, the temperature could be modified to be able to potentially raise the optimum fermenting temperature, which can allow for the wine to be fermented even with the rising climate.

It is further contemplated that the small size of the chips, which are approximate the size of a credit card, will allow for the system to be used in parallel as well. Therefore, having a large number or even any number of chips operating at the same time and with different variable inputs will allow multiple test to be accomplished at a single time. Once the beverages have been fermented, the samples produced can then be tested using conventional analytical methods for alcohol content, sugar content, and other acidity levels to determine whether the finished product is of acceptable quality.

www.manaraa.com

Furthermore, due to the flexibility of the system, a large number of yeast could be tested to determine the different qualities. For example, approximately 100 types of yeast are commercially available, and each in part is specific character to a fermented beverage, such as wine. However, due to previous studies, it has been shown that only certain types of yeast can be utilized with certain grapes. However, utilizing the beverage fermenting system of the invention will allow for a greater combination of yeast and grapes to be tested to determine whether others are acceptable to produce a quality product. The same can be said with temperature, wherein additional temperatures, not previously utilized, can be tested to determine how and if they could affect the overall product and/or quality of the product.

The optimum yeast and temperature parameters determined with the beverage fermenting apparatus and system will be implemented in several larger batch of wine (~25 liters) to evaluate how the results obtained with the invention compare with larger batches, in terms of aroma and acidity.

Therefore, a miniaturized, continuous flow beverage fermenting system, apparatus, and method has been shown and described here. It should be appreciated that the figures and descriptions herein are shown for exemplary purposes, and are not to be limiting to the overall invention. For example, as mentioned, the shapes, sizes, and configurations of many of the components can be varied, while still being within the scope of the invention.

Exemplary Claims

1. A miniaturized, continuous flow beverage fermenting apparatus, comprising:

a housing comprising a first plate and a second plate, said first plate including a channel;

a hydrophilic material generally adjacent the first plate;

a hydrophobic material generally adjacent the second plate; and

www.manaraa.com

wherein the hydrophilic and hydrophobic materials are separated to allow year to be positioned therebetween.

2. The apparatus of claim 1, wherein said second plate comprising a plurality of exhaust apertures therethrough.

3. The apparatus of claim 2, further comprising a PDMS layer around the outer perimeters of the first and second plates and positioned generally between the plates.

4. The apparatus of claim 3, wherein the exhaust apertures and channels are at least partially aligned with one another.

5. The apparatus of claim 1, wherein said first plate includes an entry aperture and an exit aperture.

6. The apparatus of claim 5, where in the channel of the first plate is serpentine-shaped.

7. The apparatus of claim 1, wherein the channel is positioned at an interior side of the first plate and extends towards but not to the exterior side of the first plate.

8. A system for making a fermented beverage, the system comprising:

a housing comprising a first plate and a second plate, said first plate including a channel, a hydrophilic material generally adjacent the first plate, and a hydrophobic material generally adjacent the second plate;

a yeast positioned generally between the hydrophilic and hydrophobic materials;

a fluid distribution system to provide a fluid to and through the channel of the first plate to allow the fluid to interact with the yeast; and

at least one sensor operatively connected to the fluid distribution system to determine characteristics of the fluid as it moves through the housing.

www.manaraa.com

9. The system of claim 8, further comprising a temperature control operatively connected to the fluid distribution system to alter the temperature of the fluid as it moves through the housing.

10. The system of claim 9, wherein the fluid distribution system comprises a fluid reservoir, a first tube to an inlet of the housing, and a second tube from an exit of the housing.

11. The system of claim 10, wherein the fluid distribution system further comprises at least one pump for moving the fluid through the system.

12. The system of claim 11, wherein the pump comprises a hydrostatic pump.

13. The system of claim 8, wherein the yeast comprises a cartridge that is positioned within the housing.

14. They system of claim 8, further comprising a PDMS layer around the outer perimeters of the first and second plates and positioned generally between the plates.

15. The system of claim 8, wherein the second plate of the housing comprises an exhaust to allow gases to escape.

16. A method of making a fermented liquid with a miniaturized, continuous flow beverage fermenting apparatus, the method comprising:

providing a housing comprising a first plate and a second plate, said first plate including a channel, a hydrophilic material generally adjacent the first plate, a hydrophobic material

generally adjacent the second plate, and a yeast positioned generally between the hydrophilic and hydrophobic materials;

circulating a liquid through the channel of the first plate of the housing and adjacent the yeast; and

determining the alcoholic content of the liquid as it is circulated through the channel to obtain a predetermined level of alcohol content to obtain the fermented liquid.

The method of claim 16, further comprising varying an input of the apparatus to obtain a different fermented liquid.

www.manaraa.com

17. The method of claim 17, wherein the varied input comprises a variation of temperature.

18. The method of claim 17, wherein the varied input comprises a different type of yeast.

19. The method of claim 16, further comprising obtaining an amount of the fermented liquid that is less than 5 mL.

Experiments and Simulation on Winery Prototype #2

Fig. 21 shows a schematic plot of prototype #2 of the microwinery, where the chamber for storing yeasts is fabricated on the bottom chip. Both top and bottom chips are made of polymethyl methacrylate (PMMA). The grape juice flows in the micro-winery through the inlet of top chip and out through the outlet. A chamber for storing yeasts is made in the bottom chip. Between the top and bottom chip is a porous hydrophilic membrane, which allows juice goes into the chamber to feed the yeasts but prevents yeasts from going inside the juice flow channel. Thus, pure grape juice can be circulated in channel and tubings without yeasts mixed in. Several through holes are made in the bottom chip for allowing the released CO2 from fermentation to goes out of the micro-winery. A porous hydrophobic membrane is placed on the bottom of yeasts chamber, which only enables CO_2 pass through, but keep juice and yeasts stay in the chamber. Two o-rings are places in between of the PMMA chips to prevent leaking. Screws are used for tighten two chips of the micro-winery.

www.manaraa.com

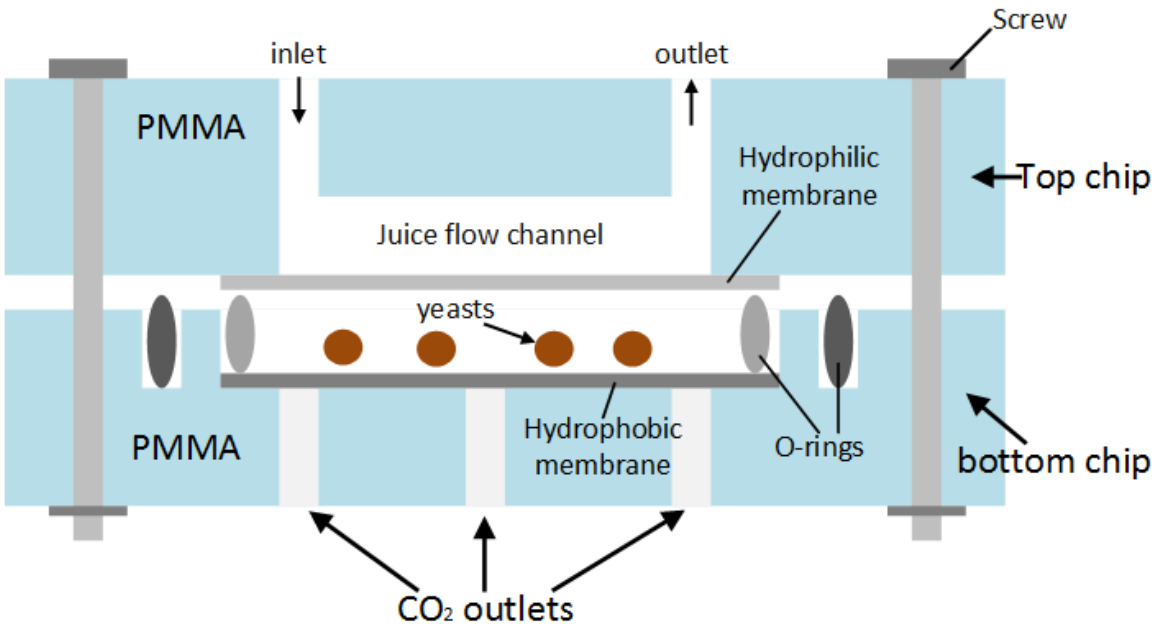

Figure 21: Schematic plot of microwinery prototype #2

This micro-winery is designed in AutoCAD, and fabricated with a milling machine. The channel in the top chip is 2 mm-wide and 0.2 mm-deep, the distance between channels is 2 mm. The depth of yeasts chamber in bottom chip is 0.6 mm, the diameter of the chamber is 47.5 mm, but only the area created by the 43 mm-diameter O-ring is used for storing yeasts and juice. The diameter of outer groove for another O-ring is 56 mm. the porous hydrophilic membrane we used in the micro-winery is 0.01 mm thick, with 0.4 µm-diameter pores. The porous hydrophobic membrane is 0.2 mm thick with pore size of 0.1 µm. The system overview of using this prototype #2 microwinery is shown below in Fig. 22.

www.manaraa.com

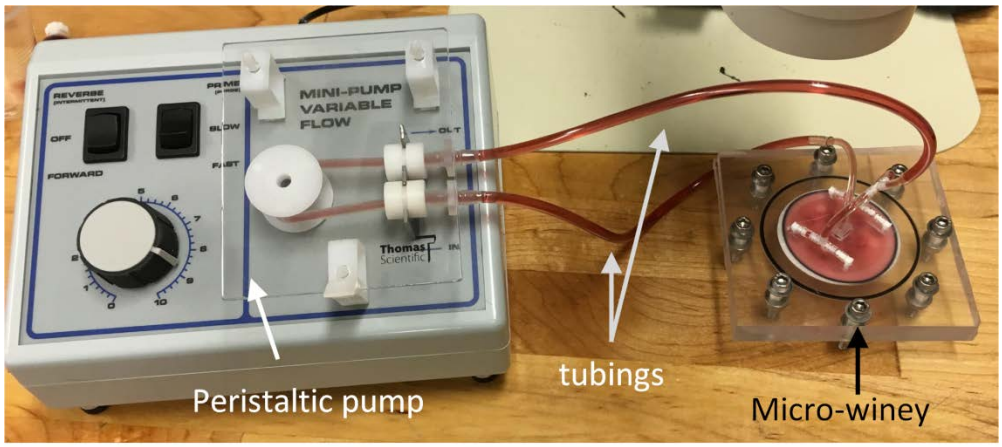

Figure 22: System overview with microwinery prototype #2.

A simulation for fermentation of grape juice in prototype #2 microwinery is performed utilizing matlab. During sugar transferring, diffusion happens within the hydrophilic membrane and convection happens around that membrane. The equations of diffusion and convection respectively are:

Diffusion equation: $\dot{m}_{dif} = \Delta C \Big/ \frac{L}{D_{AB} \times A}$

Convection equation: $\dot{m}_{con} = \Delta C \Big/ \frac{1}{h_D \times A}$

Let's consider ṁ as current I, ΔC as voltage V, we can build an equivalent circuit for modeling the mass transfer, with $R_{dif} = \frac{L}{D_{AB} \times A}, R_{con} = \frac{1}{h_D \times A}$. In order to calculate h_D, the Sherwood Number is needed. The Sherwood Number is defined as: $sh = \frac{h_D dp}{D}$, and the sherwood Number is:

$$sh = 0.3 + \frac{0.62\,\mathrm{Re}^{1/2}\,Sc^{1/3}}{[1+(0.4/Sc)^{2/3}]^{1/4}}[1+(\frac{\mathrm{Re}}{282000})^{5/8}]^{4/5} \quad \text{at } Sc\,\mathrm{Re} \geq 0.2$$

Where Re is the Reynolds Number: $\mathrm{Re} = \frac{u_r dp}{v}$, and Sc is the Schmidt Number: $Sc = \frac{v}{D}$.

The υ here is the fluid viscosity; D is the diffusion coefficient of water and sugar; dp is the hydraulic diameter; and ur is the relative velocity.

www.manaraa.com

The sugar concentration in juce is 21 Brix, which equals to 210 kg/m3. The diffusion coefficient of water and sugar is $D_{sugar/water} = 6\times10^{-10} m^2/s$. The density of pure Ethanol is $\rho_{OH} = 0.789\times10^3 kg/m^3$. The molar mass ratio of ethanol to sugar cells: 92/180. The viscosity of juice is $v_{kinimatic} = \frac{viscosity_{dynamic}}{density_{juice}} = \frac{2\times10^{-3}}{1097.3} = 1.822\times10^{-6} m^2/s$ at 22.9 Bx and 20 Celsius degree. Yeast diameter is $5\times10^{-6} m$, and assume yeasts packing ratio is 70%. Sugar Consumption per yeast cell is $I_{yeast} = 2.0278\times10^{-17} kg/s$. Thus, the total sugar consumption rate equals sugar consumption rate per yeast cell times number of yeast cells, which can be calculated by yeast diameter and packing ratio in the reactor volume.

Assume the total juice volume we use: $4mL = 4\times10^{-6} m^3$, and the flow rate set as $2.423\times10^{-8} m^3/s$. We can derive the resistance of One Pore: $R_{pore} = 5.305\times10^{15} s/m^3$. The resistance of diffusion should be: $R_{dif} = \frac{R_{pore}}{N_{pore}\times A_{pore}} = 1.4737\times10^6 s/m^3$, and the resistance of convection is $R_{con} = \frac{1}{h_D \times A_{reactor}} = 1.68\times10^7 s/m^3$.

When fermentation starts, we assume yeasts are activated and no sugar is in the reactor. The speed of sugar passing through membrane and entering reactor equals the concentration difference divided by total resistance: $I_{pass} = \frac{C_{total}}{R_{total}}$. The sugar consumption rate, Icomsume equals to the minimum one of sugar entering speed and speed of which eaten by yeasts, which are Ipass and I. The remaining sugar concentration equals to the concentration of total sugar minus consumed by yeasts: $C_{remain} = C_{total} - \frac{I_{consume}\times time}{volume}$. The fermentation stops when ethanol concentration reaches up to 12% or sugar is totally consumed.

www.manaraa.com

The modeling result is shown in Fig. 17. The fermentation stops after 1.76 hours when ethanol concertation reaches 12%, and 2.47 Brix of sugar remains.

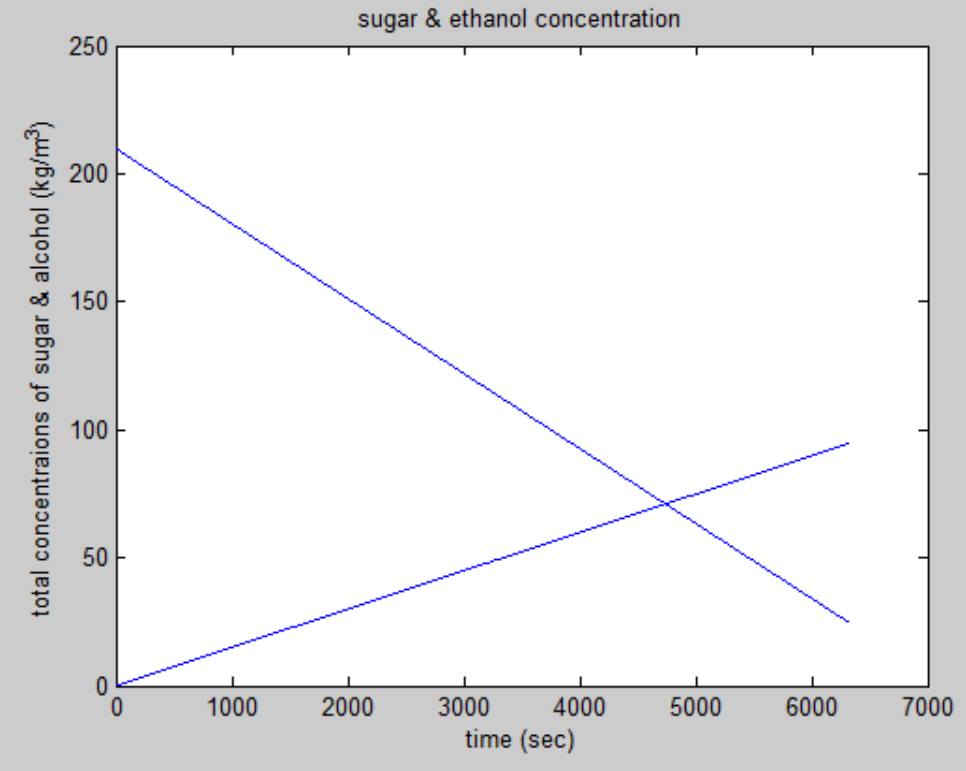

Figure 23: Matlab modelling result of grape wine fermentation.

Results and Discussion

Fig. 24 shows a measured sample made from the microwinery by high performance liquid chromatography (HPLC) in Midwest Grape and Wine Industry Institute. After three days fermentation, the ethanol percentage reaches up to 10.8% and the total remaining sugar is only 0.88%, which is good for wine making.

www.manaraa.com

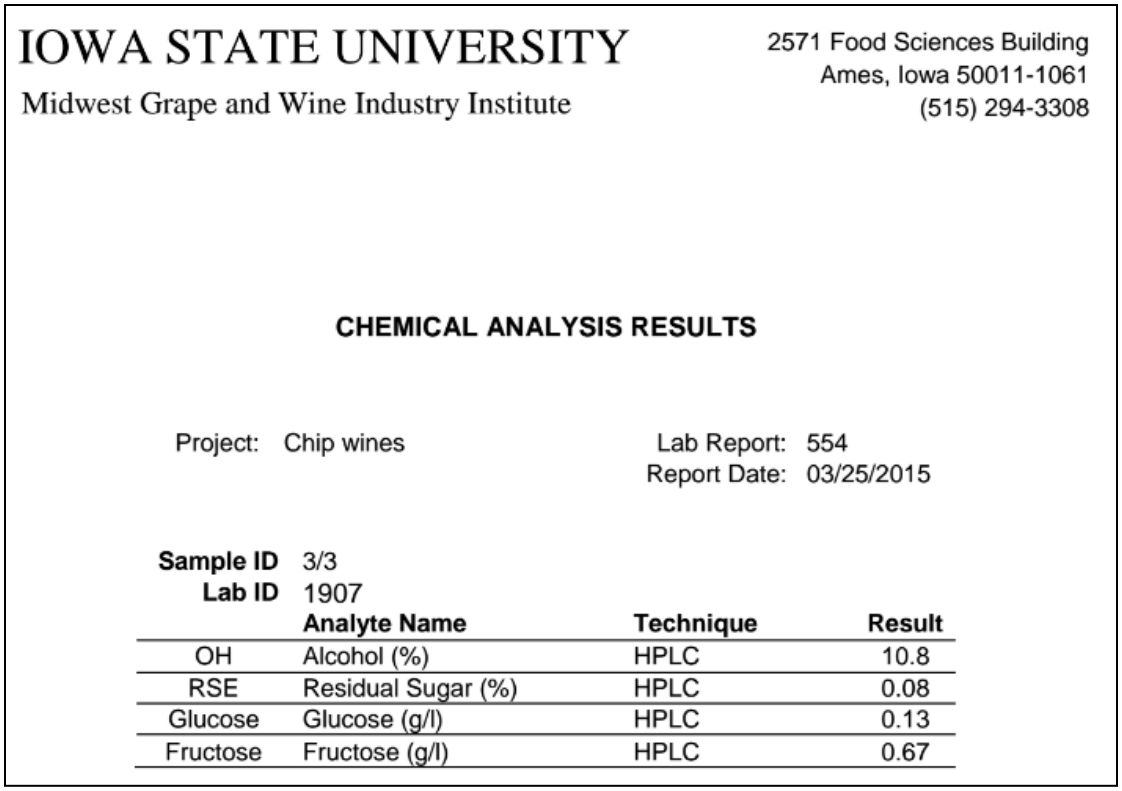

IOWA STATE UNIVERSITY

Midwest Grape and Wine Industry Institute

2571 Food Sciences Building
Ames, Iowa 50011-1061
(515) 294-3308

CHEMICAL ANALYSIS RESULTS

Project: Chip wines

Lab Report: 554
Report Date: 03/25/2015

Sample ID 3/3
Lab ID 1907

	Analyte Name	Technique	Result
OH	Alcohol (%)	HPLC	10.8
RSE	Residual Sugar (%)	HPLC	0.08
Glucose	Glucose (g/l)	HPLC	0.13
Fructose	Fructose (g/l)	HPLC	0.67

Figure 24: Chemical analysis results of one sample made by microwinery.

The future work contains analysis of the effects of different juices, yeasts, and fermentation environments on the quality of wines.

References

[1] Ronnie, Willaert. Immobilised Living Cell Systems Modeling and Experimental Methods. 42.

[2] C.A.Zuritz. Density, viscosity and coefficient of thermal expansion of clear grape juice at different soluble solid concentrations and temperatures. Journal of Food Engineering. 2004.10.

[3] Pauline M. Doran and James E. Bailey. Effects of Immobilization on Growth, Fermentation Properties, and Macromolecular Composition of Saccharomyces cerevisiae Attached to Gelatin. April 29,1985.

www.manaraa.com

CHAPTER 5. GENERAL CONCLUSIONS

The study in Chapter 2 has shown a microfluidic droplet sorter utilizing bilayer pneumatic valves, which has a high capability due to minimal interference to biological species or microorganisms inside droplets that may accompany with electrical, optical and magnetic-based techniques. Compared to single layer pneumatic valve, our sorter has more complex fabrication processes but is particularly suitable for integration into large scale microfluidic systems that use pneumatic bilayer valves. Future work includes optimizing and modifying this sorting technology for droplets containing cells or having biochemical reactions that may introduce certain characteristic changes. The changes may be detected by transmitted light or florescent light and thus trigger sorting. Besides, we will realize an integrated large-scale microfluidic system with parallel operation of sorting to increase sorting efficiency and throughput. This may be difficult to perform without using the proposed bilayer valves-based sorting method.

Chapter 3 has shown a microfluidic impedance sensor arrays integrated on printed circuit board to improve the efficiency of electronic sensor based on electrical impedance measurement in microfluidic channels. The microfluidic devices are formed on a PCB, which simplifies the integration between microfluidic devices and electronic devices and potentially reduces costs. The concentration gradient generator and sensor array result to a data acquisition device with good throughput. Future works includes building on an electronic circuit to readout impedances of sensors on PCB.

The study of Chapter 4 has shown an invention of micro-scale winery with continuous flow. Benefiting from the fast fermentation process, the micro-scale winery will have great potential to perform rapid screening of key variables of winemaking, including the type of grape juice, the type of yeasts and the environment of fermentation. Simulation of the fermentation has

www.manaraa.com

performed and shown a rapidly process with the proposed micro-winery. The future work contains analysis of the effects of different juices, yeasts, and fermentation environments on the quality of wines.

www.manaraa.com

ACKOWLEDGEMENTS

I would first like to acknowledge the guidance of my major professor, Dr. Liang Dong and co-major professor, Dr. Daniel Attinger. They have been instrumental in motivating me in order to grow and succeed during my graduate school career.

I also would thank my colleagues Mr. Yang Tian and Miss Xinran Wang their great help with the projects on the microfluidic droplet sorter and impedance microfluidic sensor.

This work was supported in part by the Institute for Physical Research and Technology and the Plant Sciences Institute both at Iowa State University, the National Science Foundation under grants CCF-1331390 and DBI-1331390.

Lastly, I would be remiss if I did not acknowledge all the love and encouragement from my family and friends over the past three years. Without the support of all those mentioned above, none of this would have been possible.

www.manaraa.com